Arabian Journal of Geosciences (2023) 16:111
https://doi.org/10.1007/s12517-022-11149-4

ORIGINAL PAPER

Microtexture and grain size characteristics of lagoonal and riverine coastal deposits along the southeastern coast of Sri Lanka: implication for paleoenvironment

Chaturanga Sandaruwan[1] · Nadeesha Madugalla[2] · Madurya Adikaram[2] · Amarasooriya Pitawala[1,3] · Tharanga Udagedara[4]

Received: 1 September 2022 / Accepted: 22 December 2022

Abstract

Beach placers are concentrations of economically potential minerals formed by surface earth processes and are identified as one of the most easily exploitable mineral deposits in the world. We studied the placer and non-placer sediments in lagoonal and riverine beaches of the southeastern part of Sri Lanka to unravel their specific sedimentary features, depositional settings and paleoenvironments. Swash zone deposits (105) were investigated for their surface microtextures, granulometry and their identification. Near the lagoonal outlets, black-coloured placers are reported with abundant ilmenite and accessory zircon, while red-coloured almandine placers are founded in the riverine areas. Placer deposits are composed of coarse-skewed leptokurtic to platykurtic fine sand and evidenced for dominant bottom suspension mechanisms on the weak wave-generated depositional agent. Quartz grains (240) from placer and siliciclastic sediments showed the presence of 25 pre-defined microtextures indicating the influences from sub-aqueous beach, fluvial, aeolian and chemical alteration processes. From siliciclastic to red placer to black placer sediments, decreasing order of source-sink distance and increasing order of fluvial influences are resulted. Cracks and solution pits are higher in the sediments of placer deposits revealing their deposition in the steady low energy environment. The crosscut relations indicate prevailed pre-aeolian processes and post-chemical alteration processes on placer deposits. Large conchoidal fractures, arcuate and straight steps microtextures, and mineralogical contents of the placer deposits infer the crystalline rock sources of granitic gneiss and garnet-bearing granulites of the Precambrian Vijayan Complex and Highland-Vijayan tectonic boundary zone.

Keywords Beach placers · Ilmenite · Microtexture · Paleoenvironment · Quartz grains · Southeast coast of Sri Lanka

Introduction

Sediments in coastal deposits are transported by various natural agents, such as glacial, fluvial, sub-aqueous beach, marine and aeolian processes prior to the deposition (Costa et al. 2013; Li et al. 2021; Mahaney 2002; Vos et al. 2014). It is significant to address these sedimentary cycles as these processes concentrate varieties of economically valuable minerals and metals such as gold, cassiterite, platinum, diamonds, ilmenite, rutile, monazite, zircon and garnet (Best 2015; Cardona et al. 2005; Mohammad et al. 2020). The "beach placers" are largely composed of resistant heavy minerals that are deposited along the edge of large water bodies and are formed due to the gravity separation processes (Haldar 2013; Haldar and Tišljar 2014; Rao et al. 1993). Such heavy minerals are often derived due to the weathering and erosional process of parent rocks that occur in the upland

Responsible editor: Attila Ciner

Highlights
- Lagoonal coastal placers are titanium placers with byproducts of zircon and almandine.
- Titanium placers are bottom-suspended fine sand that has been deposited under low-turbulence conditions.
- Microtextural tracers show multiple sedimentary episodes on quartz sediments.
- Precambrian Vijayan crust source for placers laid on the southeast coast, Sri Lanka.

✉ Nadeesha Madugalla
nadeeshamadugalla@seu.ac.lk

Extended author information available on the last page of the article

Published online: 19 January 2023

mountains, river basins and bar lagoons (Best 2015; Hoshino et al. 2016; Mohammad et al. 2020; Wang et al. 2014). Sediment deposition in coastal environments is controlled by geomorphology of beach, source-sink distance, nature of the source, transporting and depositional agents (Naidu et al. 2016; Trenhaile 2005).

Mineral grain surface textures and grain size distribution (GSD) of sediments have been used to identify their origin, transport and depositional processes, and paleoenvironmental history (Armstrong-Altrin and Natalhy-Pineda 2014; Azidane et al. 2021; Hossain et al. 2020; Mohammad et al. 2020; Pradhan et al. 2020; Rajganapathi et al. 2013; Ramos-Vázquez and Armstrong-Altrin 2020; Sinha et al. 2022). Quartz grains have largely been used for surface microtextural studies owing to their abundancy in all sedimentary environments, weathering resistance and enhanced preservability of surface microtextures (Cardona et al. 2005; Li et al. 2021; Palleyi et al. 2015; Ramos-Vázquez and Armstrong-Altrin 2020; Vos et al. 2014). The good number of research literatures have identified that the microtextures are in mechanical, chemical and mechanical-chemical origin, and have been applied to discriminate sedimentary environments (Li et al. 2021; Mahaney et al. 2001; Vos et al. 2014).

India is one of leading countries in the exploration and exploitation of coastal placer deposits (Cheepurupalli et al. 2012; Mohammad et al. 2020). The microtextural and the GSD characteristics of sediments along the Indian coast have been discussed in depth by many commendable studies (Mohammad et al. 2020; Pradhan et al. 2020; Rajganapathi et al. 2013; Rajmohan et al. 2016; Silpa et al. 2016; Udayaganesan et al. 2011). Sri Lanka, being an island at the junction of the east and west coasts of the Indian subcontinent, is gifted with beach placers. The major Sri Lankan placer deposits are (i) ilmenite deposits at Pulmoddai, Mulativu, Nayaru, Vakarei and Verugal (northeast coast of Sri Lanka); (ii) garnet deposits at Dondra, Dikwella, Ambalantota, Godawaya and Kirinda (south coast of Sri Lanka) and (iii) monazite deposits at Beruwala [southwest coast of Sri Lanka (Amalan et al. 2018; Cooray 1984; Jinadasa and Wijayadeva 2013; Mathavan and Dissanayake 1977; Subasinghe et al. 2021)]. For instances, in 2019, Sri Lanka exported 17,704 tonnages of raw ilmenite, 3173 tonnages of rutile and 1270 tonnages of zircon (Subasinghe et al. 2021). Amalan et al. (2018) interpreted that the Precambrian metamorphic basement composed of high-grade metamorphic rocks may have been the source for many of these deposits, while Subasinghe et al. (2021) suggested that these northeastern deposits are naturally conserved due to annual replenishment during the northeast monsoon. Although, the southeast (SE) coast of Sri Lanka comprises of extensive depositional beaches, chains of lagoons, estuaries and underlain by mineralogically divers Vijayan Complex (VC) metamorphic basement, a very few published records are available on the transportation and depositional characteristics of beach placers exposed along the SE coast of Sri Lanka (Cooray and Katupotha 1991; Narvekar and Kumar 2006; Weerakkody 1985).

This work explore the heavy mineral concentrated areas along the lagoonal and riverine beaches of the southeastern coast of Sri Lanka. The study is significant and has objectives to differentiate origin, paleoenvironment, transport and deposition processes of heavy placers from siliciclastic deposits. The study results guide for explore renewable ilmenite and garnet placer deposits exposed along lagoonal and riverine beaches across the continents.

Study area

The studied beach sediments are exposed along the SE coast of Sri Lanka. (7° 16′ 16.1″ N–81° 52′ 03.5″ E and 6° 44′ 49.1″ N–81° 48′ 37.5″ E; Fig. 1). The SE beach consists of coastal dunes, lagoon outlets, river outlet, crescent-shaped bays, sandy spits and rocky headlands (Fig. 2; Richmond et al. 2006; Satyanarayana et al. 2017; Weerakkody 1985). These lagoon and river outlets occur between two adjacent headlands that control the bay morphology (Richmond et al. 2006). Ambalam Oya (86×10^6 m^3year^{-1}), Karanda Oya (241×10^6 m^3year^{-1}), Heda Oya (372×10^6 m^3year^{-1}) and Wil Oya (236×10^6 m^3year^{-1}) are the major rivers that bring fresh water to the study area (Katupotha and Gamage 2020). These river basins receive higher precipitation (750 to 500 mm) during the northeast monsoon and second intermonsoon periods, from October to February. The Heda Oya flows directly into the sea and other freshwater sources flow into lagoons, namely Periya Kalappuwa lagoon (139×10^6 m^3year^{-1}), Korai lagoon complex (45×10^6 m^3year^{-1}), Komari lagoon, Pothuvil lagoon (213×10^6 m^3year^{-1}), Arugam Kalappuwa lagoon (394×10^6 m^3 $year^{-1}$) (Silva et al. 2013). These lagoon entrances are 220, 120, 110, 170 and 410 m long respectively (Silva et al. 2013).

The study area is underlain with hornblende-biotite gneiss, migmatite, charnockitic gneiss and granitic gneiss of the VC (Silva et al. 2013). The river basins display the VC Precambrian metamorphic basement (ca. 1.0–1.8 Ga) (Cooray 1984; Milisenda et al. 1988). The VC basement commonly consists of granitic gneisses, migmatites and biotite-hornblende gneisses with minor charnockitic gneisses and meta-sediments scattered bands (Cooray 1994; Kehelpannala 1997). Few dolerite intrusions also exposed in these river basins (Arachchi et al. 2017). The Wila Oya and Heda Oya rivers start from the Highland-Vijayan tectonic mixed zone, where serpentine bodies and iron ore deposits are present (Manjula et al. 2020; Rajapaksha et al. 2012).

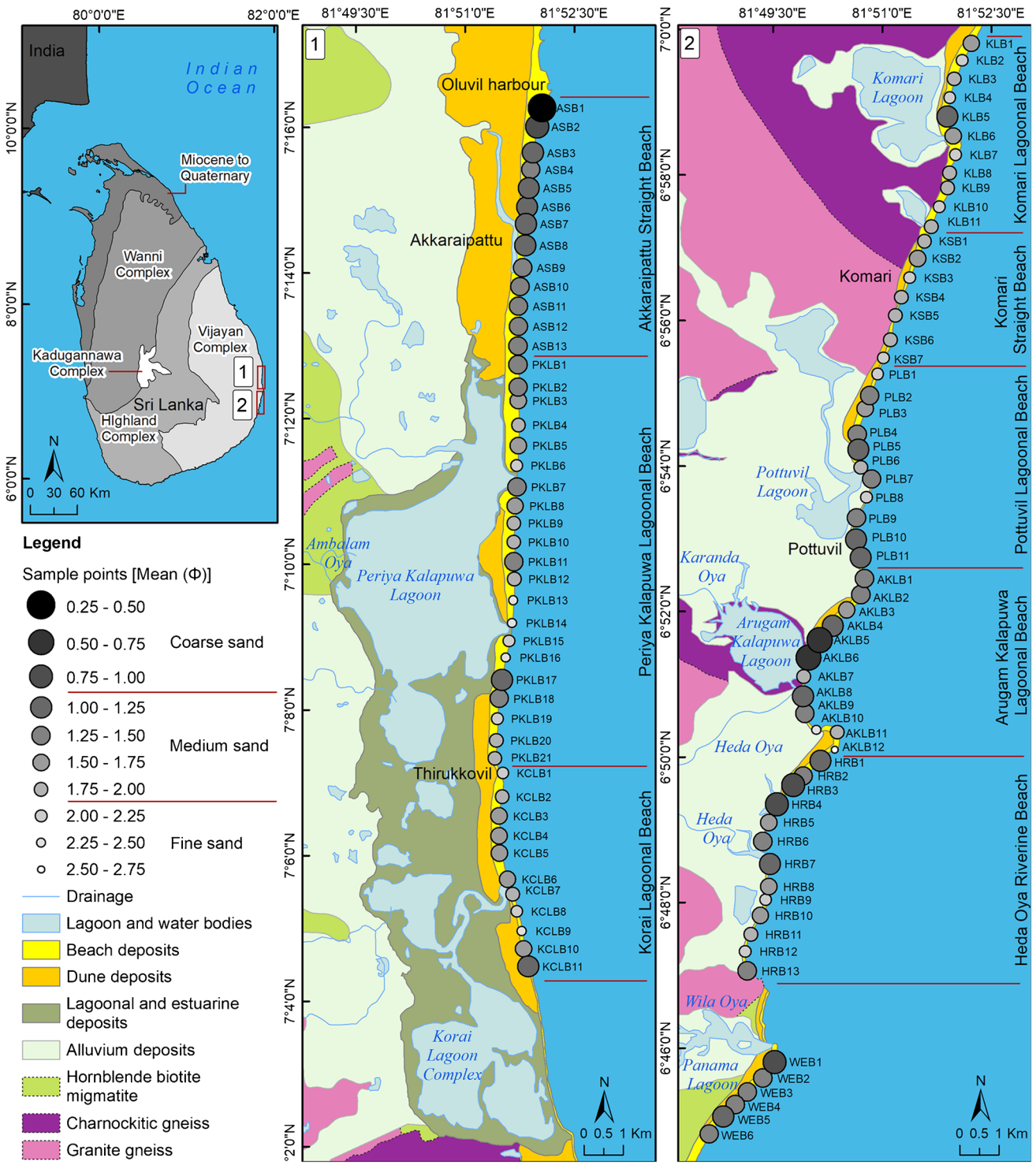

Fig. 1 The sample location map of the study area showing the geology and lithotectonic units of Sri Lanka (after Cooray 1994)

Materials and methods

Samples were taken from October 2019 to February 2020 considering the peak river discharge period of the year. The lagoonal beaches (Periya Kalapuwa, Korai, Komari, Pottuvil, Arugam Kalapuwa) and Heda Oya riverine beach were selected to explore the heavy placer deposits (Fig. 1). After field observations of black-coloured placers in lagoonal areas and red-coloured placers in riverine areas, samples were taken in both beach environments up

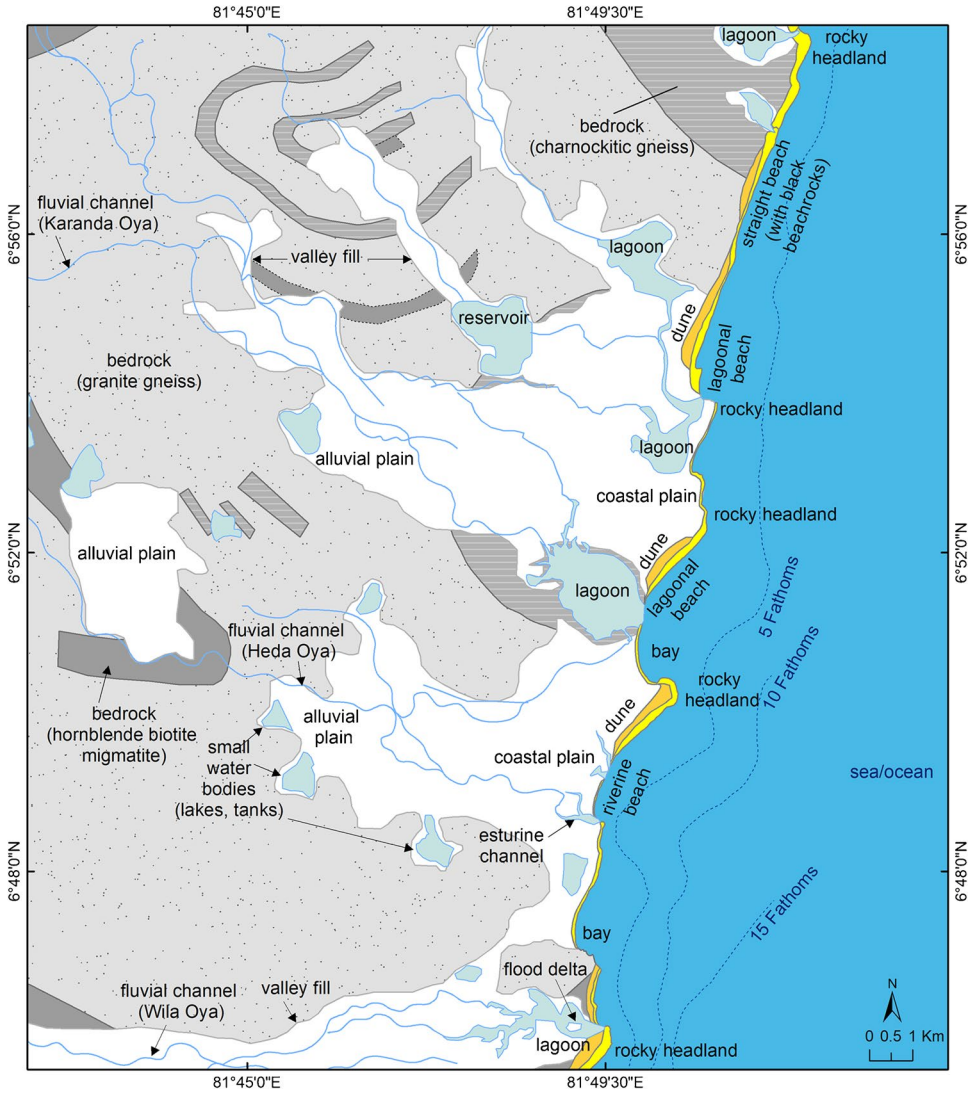

Fig. 2 The coastal landform distribution of fluvial channels, estuarine channels, alluvial plains, coastal plains, bedrock geology, lagoons, bay morphologies, rocky headlands and coastal dunes along the beach environments in SE coast, Sri Lanka

to 2–3 km length from the outlets. The sediments were collected with the aid of a plastic shovel and care was taken to prevent anthropogenic contents. To understand the effects of fluvial and coastal processes on sediments, a different set of samples was fetched from straight beaches (Akkaraipattu, Komari) that are more than 3 km away from fluvial outlets. In total, 105 samples were collected from different riverine, lagoonal and straight coastal areas of the SE coast and their different environmental impacts, textural and mineralogical characteristics were understood. The samples were bagged with a 0.5-km interval and to a depth of 15–30 cm from the middle of the swash zone (Fig. 1).

Granulometry

Sieving technique is applied to the sediment sample to interpret the GSD parameters. First, 100 g of representative sediment fractions were processed by the coning and quartering method (Rajganapathi et al. 2013). The 10% HCl solution and deionized water were used to remove carbonate and salt coatings on the sediments (Rajmohan et al. 2016; Rosas et al. 2014). Thereafter, the treated samples were dried in an oven at 60 °C for 24 h. The samples were analysed at 1 ϕ interval through ASTM sieves for 15 min using a Retsch vibratory sieve shaker (AS 200 digit Folk and Ward 1957; Sinha et al. 2022). The mean (M_Z), sorting (σ_1), skewness (Sk_1) and kurtosis (K_G) were evaluated using the Gradistat excel template following the Folk and Ward (1957) method (Blott and Pye 2001).

Reasoning of grain surface microtexture

Twelve numbers of uniform lagoonal, riverine and straight beach sediments were investigated in the SEM instrument to its microtextures to decipher the sedimentation history.

Vos et al (2014) and J. Li et al (2021) methods followed in preparation of sediments for SEM analysis. The isolated quartz grains (240) were examined using the SEM (ZEISS EVO LS15) at Department of Geology, University of Peradeniya, Sri Lanka. The samples were studied under magnification from × 100 to × 5000. The observed microtextures were quantitatively divided into five categories: abundant (*A*, > 75% of grains), common (*C*, 50–75%), sparse (*S*, 5–50%) and rare (*R*, < 5%) (Vos et al. 2014). Environmental discrimination scheme proposed by Vos et al. (2014) was used to construct the paleoenvironments of sedimentary deposits.

Mineral composition analysis

Mineralogical identifications of 12 types of coastal sediments were analyzed using Rigaku® RINT Ultima III X-ray diffraction (XRD) instrument at Department of Applied Earth Sciences, Uwa Wellassa University, Sri Lanka. The XRD patterns were noted between 15° and 85° (2θ).

Results and discussion

Field observations

The majority of Sri Lanka's southeast coast is made up of sediments that are the size of sand, such as the entire 6-km Akkaraipattu straight beach faces (Fig. 3a). On the cliffs of Komari Straight Beach, black-coloured massive sedimentary formations are revealed, with sporadic distributions. This beach features black beach rocks in addition to black thick sediments that reach roughly 2–3 km parallel to the shoreline (Fig. 3b). Each lagoonal beach has a few strewn

Fig. 3 The field view of heavy placers along the SE coast, Sri Lanka. (**a**) Siliciclastic deposits at Akkaraipattu straight beach, (**b**) black-coloured heavy placers and their cemented beach rocks at Komari straight beach, (**c**) layer thickness of heavy placers at Periya Kalapuwa lagoonal beach, (**d**) scattered distributions of black-coloured heavy placers at Pottuvil lagoonal beach, (**e**) layer thickness of heavy placers at Komari lagoonal beach, (**f**) scattered distributions of red-coloured heavy placers at riverine beach

layers of similar dark silt (Fig. 3d). Above the siliciclastic deposits, these dispersed deposits occur as strata that are 10- to 15-cm thick (Fig. 3c, e). Additionally, the Hada Oya riverine beach exhibits red sedimentary layers together with some black sediments (Fig. 3f). These layers of red sediment are situated along a 2–3-km-long beach spit.

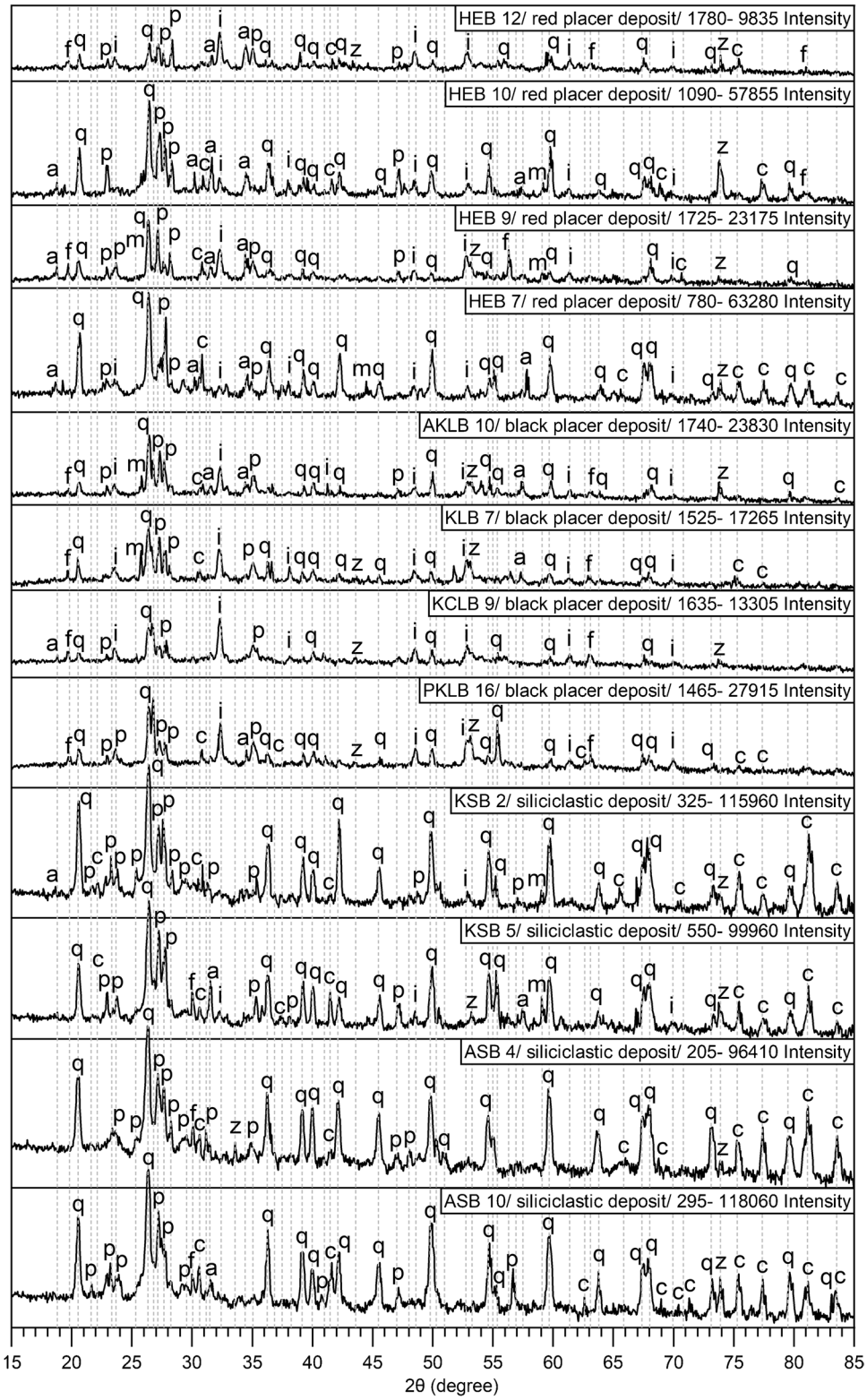

Fig. 4 The XRD spectrums of siliciclastic deposits, black- and red-coloured heavy placers in SE coast, Sri Lanka. q, quartz; p, albite; c, magnesium-calcitel i, ilmenite; a, almandine; m, monazite; z, zircon; and f, ferrihydride (after Sandaruwan et al. 2022)

Table 1 The descriptive analysis of the grain size statistical parameters that resulted for the SE coast, Sri Lanka. aQuantitative statistics in phi (Φ), bdescriptive statistics

Sample ID	Mean[a]	Sorting[a]	Skewness[a]	Kurtosis[a]	Mean[B]	Sorting[B]	Skewness[B]	Kurtosis[B]
ASB1	0.47	1.08	0.22	0.95	Coarse sand	Poorly sorted	Fine skewed	Mesokurtic
ASB2	0.97	0.79	0.24	0.90	Coarse sand	Moderately sorted	Fine skewed	Mesokurtic
ASB3	1.24	0.77	–0.04	1.03	Medium sand	Moderately sorted	Symmetrical	Mesokurtic
ASB4	1.31	0.73	–0.07	1.19	Medium sand	Moderately sorted	Symmetrical	Leptokurtic
ASB5	1.21	0.75	–0.04	1.00	Medium sand	Moderately sorted	Symmetrical	Mesokurtic
ASB6	1.23	0.74	–0.07	1.03	Medium sand	Moderately sorted	Symmetrical	Mesokurtic
ASB7	1.07	0.83	–0.01	0.96	Medium sand	Moderately sorted	Symmetrical	Mesokurtic
ASB8	1.10	0.80	–0.07	0.96	Medium sand	Moderately sorted	Symmetrical	Mesokurtic
ASB9	1.27	0.71	–0.09	1.13	Medium sand	Moderately sorted	Symmetrical	Leptokurtic
ASB10	1.34	0.72	–0.08	1.31	Medium sand	Moderately sorted	Symmetrical	Leptokurtic
ASB11	1.34	0.76	–0.08	1.28	Medium sand	Moderately sorted	Symmetrical	Leptokurtic
ASB12	1.42	0.68	–0.05	1.31	Medium sand	Moderately well sorted	Symmetrical	Leptokurtic
ASB13	1.32	0.73	–0.08	1.24	Medium sand	Moderately sorted	Symmetrical	Leptokurtic
PKLB1	1.26	0.66	–0.14	1.10	Medium sand	Moderately well sorted	Coarse skewed	Mesokurtic
PKLB2	1.47	0.76	0.00	1.30	Medium sand	Moderately sorted	Symmetrical	Leptokurtic
PKLB3	1.57	0.84	0.02	1.26	Medium sand	Moderately sorted	Symmetrical	Leptokurtic
PKLB4	1.76	0.67	0.18	1.06	Medium sand	Moderately well sorted	Fine skewed	Mesokurtic
PKLB5	1.54	0.64	0.05	1.37	Medium sand	Moderately well sorted	Symmetrical	Leptokurtic
PKLB6	2.14	0.79	0.00	0.90	Fine sand	Moderately sorted	Symmetrical	Mesokurtic
PKLB7	1.31	0.72	–0.09	1.24	Medium sand	Moderately sorted	Symmetrical	Leptokurtic
PKLB8	1.59	0.69	0.07	1.30	Medium sand	Moderately well sorted	Symmetrical	Leptokurtic
PKLB9	1.82	0.69	0.16	0.92	Medium sand	Moderately well sorted	Fine skewed	Mesokurtic
PKLB10	1.77	0.68	0.17	1.05	Medium sand	Moderately well sorted	Fine skewed	Mesokurtic
PKLB11	1.32	0.63	–0.13	1.24	Medium sand	Moderately well sorted	Coarse skewed	Leptokurtic
PKLB12	1.98	0.67	0.04	0.74	Medium sand	Moderately well sorted	Symmetrical	Platykurtic
PKLB13	2.26	0.60	–0.26	1.02	Fine sand	Moderately well sorted	Coarse skewed	Mesokurtic
PKLB14	2.25	0.59	–0.27	1.04	Fine sand	Moderately well sorted	Coarse skewed	Mesokurtic

Table 1 (continued)

Sample ID	Mean[a]	Sorting[a]	Skewness[a]	Kurtosis[a]	Mean[B]	Sorting[B]	Skewness[B]	Kurtosis[B]
PKLB15	2.16	0.67	–0.23	0.86	Fine sand	Moderately well sorted	Coarse skewed	Platykurtic
PKLB16	2.32	0.62	–0.23	1.27	Fine sand	Moderately well sorted	Coarse skewed	Leptokurtic
PKLB17	1.18	0.80	0.07	0.92	Medium sand	Moderately sorted	Symmetrical	Mesokurtic
PKLB18	1.46	0.70	–0.02	1.32	Medium sand	Moderately sorted	Symmetrical	Leptokurtic
PKLB19	2.07	0.77	–0.21	0.91	Fine sand	Moderately sorted	Coarse skewed	Mesokurtic
PKLB20	1.81	0.70	0.14	0.94	Medium sand	Moderately well sorted	Fine skewed	Mesokurtic
PKLB21	1.81	0.77	0.12	1.00	Medium sand	Moderately sorted	Fine skewed	Mesokurtic
KCLB1	2.23	0.77	–0.05	0.97	Fine sand	Moderately sorted	Symmetrical	Mesokurtic
KCLB2	1.98	0.72	0.14	0.82	Medium sand	Moderately sorted	Fine skewed	Platykurtic
KCLB3	1.64	0.73	0.09	1.28	Medium sand	Moderately sorted	Symmetrical	Leptokurtic
KCLB4	1.67	0.73	0.10	1.26	Medium sand	Moderately sorted	Symmetrical	Leptokurtic
KCLB5	1.74	0.78	0.03	0.98	Medium sand	Moderately sorted	Symmetrical	Mesokurtic
KCLB6	1.64	0.73	0.09	1.30	Medium sand	Moderately sorted	Symmetrical	Leptokurtic
KCLB7	1.96	0.69	0.15	0.79	Medium sand	Moderately well sorted	Fine skewed	Platykurtic
KCLB8	2.17	0.69	–0.14	0.91	Fine sand	Moderately well sorted	Coarse skewed	Mesokurtic
KCLB9	2.37	0.57	–0.17	1.24	Fine sand	Moderately well sorted	Coarse skewed	Leptokurtic
KCLB10	1.66	0.92	–0.12	0.88	Medium sand	Moderately sorted	Coarse skewed	Platykurtic
KCLB11	1.23	0.76	–0.08	1.02	Medium sand	Moderately sorted	Symmetrical	Mesokurtic
KLB1	1.53	0.88	–0.01	1.01	Medium sand	Moderately sorted	Symmetrical	Mesokurtic
KLB2	2.07	0.65	–0.12	0.75	Fine sand	Moderately well sorted	Coarse skewed	Platykurtic
KLB3	1.97	0.73	0.03	0.82	Medium sand	Moderately sorted	Symmetrical	Platykurtic
KLB4	2.03	0.74	–0.24	0.88	Fine sand	Moderately sorted	Coarse skewed	Platykurtic
KLB5	1.16	0.78	–0.02	0.94	Medium sand	Moderately sorted	Symmetrical	Mesokurtic
KLB6	1.68	0.75	0.08	1.20	Medium sand	Moderately sorted	Symmetrical	Leptokurtic
KLB7	2.16	0.72	–0.37	1.13	Fine sand	Moderately sorted	Strongly coarse skewed	Leptokurtic
KLB8	1.83	0.64	0.22	0.83	Medium sand	Moderately well sorted	Fine skewed	Platykurtic
KLB9	1.99	0.74	–0.18	0.86	Medium sand	Moderately sorted	Coarse skewed	Platykurtic
KLB10	2.22	0.72	–0.12	1.03	Fine sand	Moderately sorted	Coarse skewed	Mesokurtic
KLB11	1.86	0.91	–0.25	0.86	Medium sand	Moderately sorted	Coarse skewed	Platykurtic

Table 1 (continued)

Sample ID	Mean[a]	Sorting[a]	Skewness[a]	Kurtosis[a]	Mean[B]	Sorting[B]	Skewness[B]	Kurtosis[B]
KSB1	1.88	0.84	–0.11	0.88	Medium sand	Moderately sorted	Coarse skewed	Platykurtic
KSB2	1.71	0.84	–0.06	0.90	Medium sand	Moderately sorted	Symmetrical	Mesokurtic
KSB3	2.09	0.68	–0.24	0.83	Fine sand	Moderately well sorted	Coarse skewed	Platykurtic
KSB4	1.80	0.80	–0.01	0.92	Medium sand	Moderately sorted	Symmetrical	Mesokurtic
KSB5	1.97	0.77	–0.19	0.88	Medium sand	Moderately sorted	Coarse skewed	Platykurtic
KSB6	1.78	0.79	0.05	1.00	Medium sand	Moderately sorted	Symmetrical	Mesokurtic
KSB7	2.08	0.65	–0.16	0.76	Fine sand	Moderately well sorted	Coarse skewed	Platykurtic
PLB1	2.04	0.67	–0.07	0.74	Fine sand	Moderately well sorted	Symmetrical	Platykurtic
PLB2	1.48	0.80	0.00	1.19	Medium sand	Moderately sorted	Symmetrical	Leptokurtic
PLB3	1.74	0.74	0.07	1.05	Medium sand	Moderately sorted	Symmetrical	Mesokurtic
PLB4	1.32	0.72	–0.07	1.18	Medium sand	Moderately sorted	Symmetrical	Leptokurtic
PLB5	1.17	0.77	0.03	0.92	Medium sand	Moderately sorted	Symmetrical	Mesokurtic
PLB6	1.89	0.77	–0.10	0.89	Medium sand	Moderately sorted	Coarse skewed	Platykurtic
PLB7	1.30	0.63	–0.15	1.20	Medium sand	Moderately well sorted	Coarse skewed	Leptokurtic
PLB8	2.02	0.77	–0.18	0.87	Fine sand	Moderately sorted	Coarse skewed	Platykurtic
PLB9	1.32	0.68	–0.10	1.28	Medium sand	Moderately well sorted	Symmetrical	Leptokurtic
PLB10	1.08	0.66	–0.15	0.76	Medium sand	Moderately well sorted	Coarse skewed	Platykurtic
PLB11	1.03	0.72	0.10	0.83	Medium sand	Moderately sorted	Fine skewed	Platykurtic
AKLB1	1.27	0.72	–0.16	1.27	Medium sand	Moderately sorted	Coarse skewed	Leptokurtic
AKLB2	1.40	0.68	–0.06	1.31	Medium sand	Moderately well sorted	Symmetrical	Leptokurtic
AKLB3	1.71	0.76	0.09	1.15	Medium sand	Moderately sorted	Symmetrical	Leptokurtic
AKLB4	1.15	0.73	–0.05	0.91	Medium sand	Moderately sorted	Symmetrical	Mesokurtic
AKLB5	0.50	0.67	0.01	1.31	Coarse sand	Moderately well sorted	Symmetrical	Leptokurtic
AKLB6	0.65	0.63	0.11	1.27	Coarse sand	Moderately well sorted	Fine skewed	Leptokurtic
AKLB7	1.94	0.68	–0.02	0.79	Medium sand	Moderately well sorted	Symmetrical	Platykurtic
AKLB8	1.02	0.64	–0.04	0.74	Medium sand	Moderately well sorted	Symmetrical	Platykurtic

Table 1 (continued)

Sample ID	Mean[a]	Sorting[a]	Skewness[a]	Kurtosis[a]	Mean[B]	Sorting[B]	Skewness[B]	Kurtosis[B]
AKLB9	1.43	0.67	–0.06	1.33	Medium sand	Moderately well sorted	Symmetrical	Leptokurtic
AKLB10	2.27	0.72	–0.23	1.41	Fine sand	Moderately sorted	Coarse skewed	Leptokurtic
AKLB11	1.96	0.69	0.11	0.77	Medium sand	Moderately well sorted	Fine skewed	Platykurtic
AKLB12	2.55	0.59	0.03	1.34	Fine sand	Moderately well sorted	Symmetrical	Leptokurtic
HRB1	1.21	0.76	–0.08	1.02	Medium sand	Moderately sorted	Symmetrical	Mesokurtic
HRB2	1.45	0.85	0.00	1.15	Medium sand	Moderately sorted	Symmetrical	Leptokurtic
HRB3	0.93	1.02	–0.12	0.98	Coarse sand	Poorly sorted	Coarse skewed	Mesokurtic
HRB4	0.94	0.65	0.05	0.74	Coarse sand	Moderately well sorted	Symmetrical	Platykurtic
HRB5	1.74	0.66	0.17	1.10	Medium sand	Moderately well sorted	Fine skewed	Mesokurtic
HRB6	1.36	0.77	–0.04	1.13	Medium sand	Moderately sorted	Symmetrical	Leptokurtic
HRB7	1.17	0.78	–0.04	0.94	Medium sand	Moderately sorted	Symmetrical	Mesokurtic
HRB8	1.62	0.89	–0.04	0.89	Medium sand	Moderately sorted	Symmetrical	Platykurtic
HRB9	2.08	0.65	–0.19	0.77	Fine sand	Moderately well sorted	Coarse skewed	Platykurtic
HRB10	1.74	0.74	0.06	1.05	Medium sand	Moderately sorted	Symmetrical	Mesokurtic
HRB11	1.99	0.70	–0.15	0.82	Medium sand	Moderately well sorted	Coarse skewed	Platykurtic
HRB12	2.12	0.62	–0.21	0.80	Fine sand	Moderately well sorted	Coarse skewed	Platykurtic
HRB13	1.34	0.93	0.05	0.86	Medium sand	Moderately sorted	Symmetrical	Platykurtic
WEB1	0.78	1.00	0.02	0.96	Coarse sand	Moderately sorted	Symmetrical	Mesokurtic
WEB2	1.32	0.76	–0.07	1.17	Medium sand	Moderately sorted	Symmetrical	Leptokurtic
WEB3	1.45	0.86	0.00	1.12	Medium sand	Moderately sorted	Symmetrical	Leptokurtic
WEB4	1.37	0.76	–0.04	1.21	Medium sand	Moderately sorted	Symmetrical	Leptokurtic
WEB5	1.07	0.71	0.01	0.83	Medium sand	Moderately sorted	Symmetrical	Platykurtic
WEB6	1.43	0.96	0.10	0.78	Medium sand	Moderately sorted	Symmetrical	Platykurtic

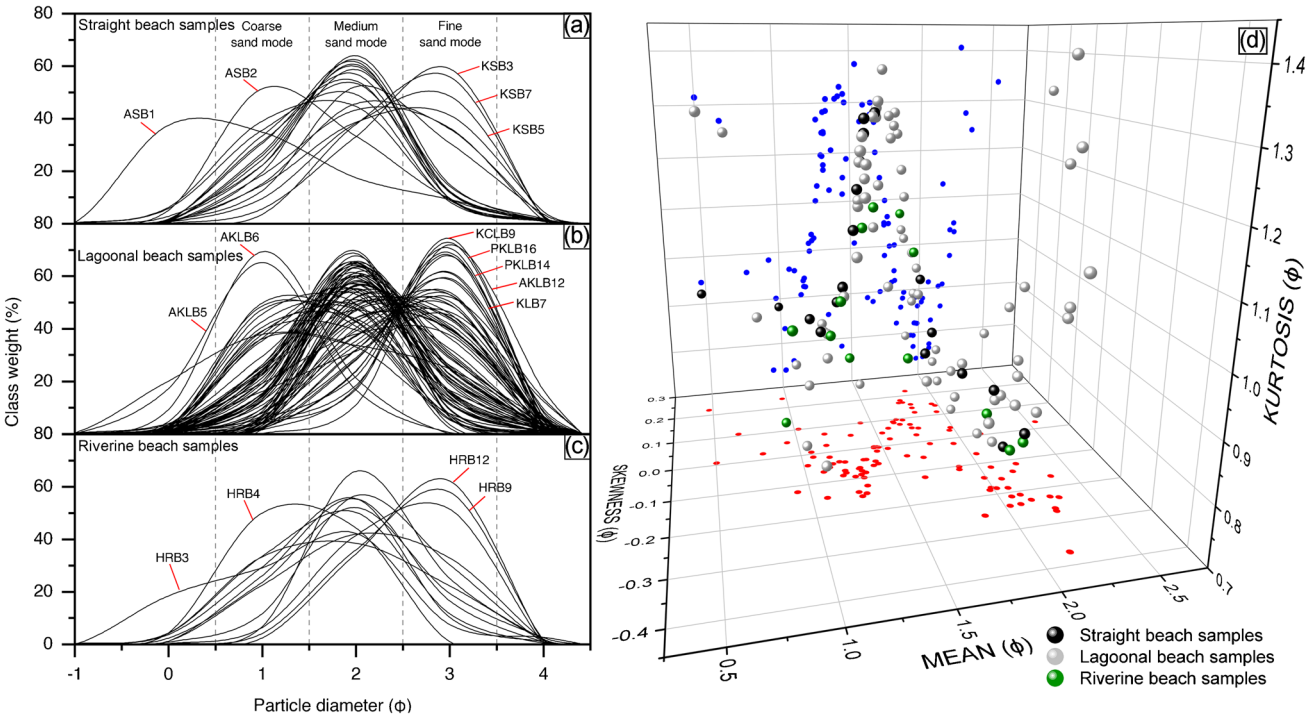

Fig. 5 The GSDs of surface sediments in SE coast, Sri Lanka. Sediment populations show major three different modes around 1.5–2.5 phi (medium sand mode), 2.5–3.5 phi (fine sand mode) and 0.5–1.5 phi (coarse sand mode). (**a**, **b**, **c**) Grain size distributions in straight, lagoonal and riverine beach samples; (**d**) mean, skewness and kurtosis tri-variate scatter graph. Helical projections of sinusoidal trends are shown in red and blue colour dots

Precious minerals in coastal placer deposits

According to the XRD investigations, the sediments obtained from straight beach faces are primarily made up of the minerals quartz, albite and magnesian calcite (Fig. 4). In addition, the accessary phases ilmenite, zircon, monazite, almandine and ferrihydride can be found. As a result, these sediments are referred to as "siliciclastic deposits" moving forward.

The XRD investigations of the black and red deposits from lagoonal and riverine beaches revealed that those are composed of ilmenite, almandine and zircon (Fig. 4). The peak intensities of quartz, albite and magnesium-calcite of these sediments are very low compared to the siliciclastic sediments. For example, quartz peaks at 20.85, 26.65, 36.50, 50.14, 59.96 and 68.15 (2θ values) clearly indicate the low abundance of quartz in these sediments. Therefore, these sediments are hereafter identified as "heavy placer minerals".

The black-coloured placers are composed of quartz, albite, ilmenite and zircon. Peaks at 32.40 and 53.30 2θ show higher concentrations of ilmenite in black placer deposits. Almandine, ferrihydride, monazite and magnesium-calcite are referred as accessory minerals. These heavy minerals are associated with high temperature rocks such as granitic gneiss, granodioritic gneiss and charnokites (Ng et al. 2017; Van-Gosen et al. 2014). Hence, it can be justified that the crystalline rocks of VC might be the source for the above placers.

The red-coloured placers are composed of quartz, albite, almandine, ilmenite, zircon and magnesium-calcite. The peaks at 18.78 and 34.60 2θ indicate the presence of almandine in the red placer deposits. The source of the almandine in these red placer deposits may be garnet-bearing granulites in the Highland-Vijayan tectonic mixed zone, which is the upper catchment area of Heda Oya and Wila Oya rivers (He et al. 2016; Ng et al. 2017).

Evidence of deposition environments based on grain size

The dimensions of heavy placers

The results of the grain size statistical parameters are displayed in Table 1. Tri-variate and bivariate scatter graphs of grain size parameters are used to understand sandy distributions and their depositional settings (Azidane et al. 2021; Elsherif et al. 2020; Folk and Ward 1957; Rajganapathi et al. 2013). The samples from lagoonal, riverine and straight beaches are in varied grain size distributions formed under fine, medium and coarse sand patterns (Fig. 5a–c). The mean, skewness and kurtosis tri-variate scatter graph represent an approximate helical shape (Fig. 5d). Many sedimentary environments show parts of this helix and used for identifying the relative abundance of multiple sand types (Folk and Ward 1957; Inman 1949). As a result of the vertical and horizontal projections of this helix, sinusoidal scatter relations occur at bivariate plots of mean vs. skewness and mean vs. kurtosis (Fig. 5d). The mean vs. kurtosis plot resulted a sinusoidal tendency demonstrating three leptokurtic and two

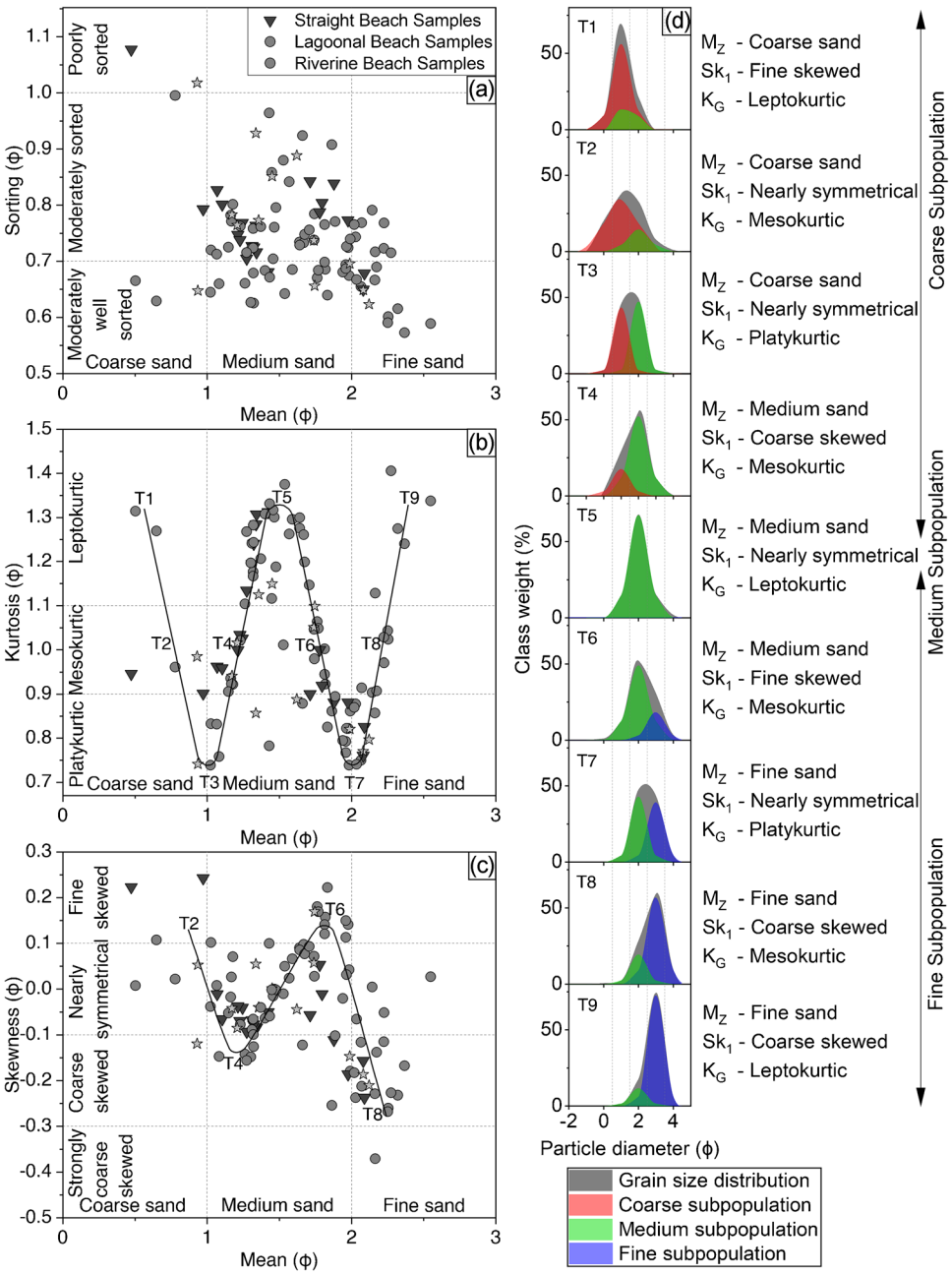

Fig. 6 The bivariate scatter plots of grain size parameters of SE coastal samples, Sri Lanka. (**a**) Mean vs. sorting scatter plot, (**b**) mean vs. kurtosis scatter plot, (**c**) mean vs. skewness scatter plot, (**d**) sandy subpopulation variations along the helical trend

platykurtic turning points associated with fine, medium and coarse sand (T1, T3, T5, T7 and T9 in Fig. 6). These leptokurtic indicate high homogeneity of the sand type, while the platykurtic show an equal abundance of the two types of sand (Elsherif et al. 2020; Folk and Ward 1957). As a result of the sinusoidal relation of skewness against mean, two fine-skewed and two coarse-skewed turning points are obtained (T2, T4, T6 and T8 in Fig. 6). The samples with skewed distribution indicate that one primary sand type with a secondary sub-population has been deposited. Hence, this helical relation indicates variations in sandy sub-populations and helps to identify variations in heavy placer deposits.

Most of the coastal samples display moderately sorted to moderately well-sorted characteristics (98% of the samples) and medium grain size (73%, (Fig. 6a)). It indicates the removal of both fine and coarse sub-population (Fig. 6). In the swash zone, fine sands are removed by aeolian processes, while hydrodynamic processes sort coarse sand near to the shoreline (Biederman 1962; Jiang et al. 2015). This suggests that many beach samples are made up of sediments from winnowing and uprush-backwash processes (Mout and Sarmah 2022; Sinha et al. 2022).

The black placers exposed in the lagoonal beaches are concentrated in the T9 region of helical trend. They are characterised by coarse-skewed-leptokurtic-find sand size distributions (Fig. 5b). The red placers exposed in riverine beach and black placer deposits in Komari straight beach are concentrated in the T7 region of the helical trend. They represent coarse-skewed-platykurtic fine sand size distributions (Fig. 5a, c). Hence, the highest uniform heavy placer deposits are occurred in the lagoonal beach environments. The deposition of coarse-skewed fine sand indicates comparatively weak turbulence processes (Azidane et al. 2021; Jiang et al. 2015; Rajganapathi et al. 2013). Bujan et al. (2019) and Mohammad et al. (2020) interpreted that the heavy placers on beach faces settle due to their higher specific gravity than siliciclastic deposits of same size, which gives higher settling capacity for winnowing processes. Hence, weak wave-generated processes and higher specific gravity may have been played a role to settle heavy placer deposits on swash zone with scattered distributions. As a rare content (6%), coarse sand samples are found with fine-skewed leptokurtic to platykurtic (Fig. 5a–c). Besides, these deposits are relatively formed under high turbulence processes and less

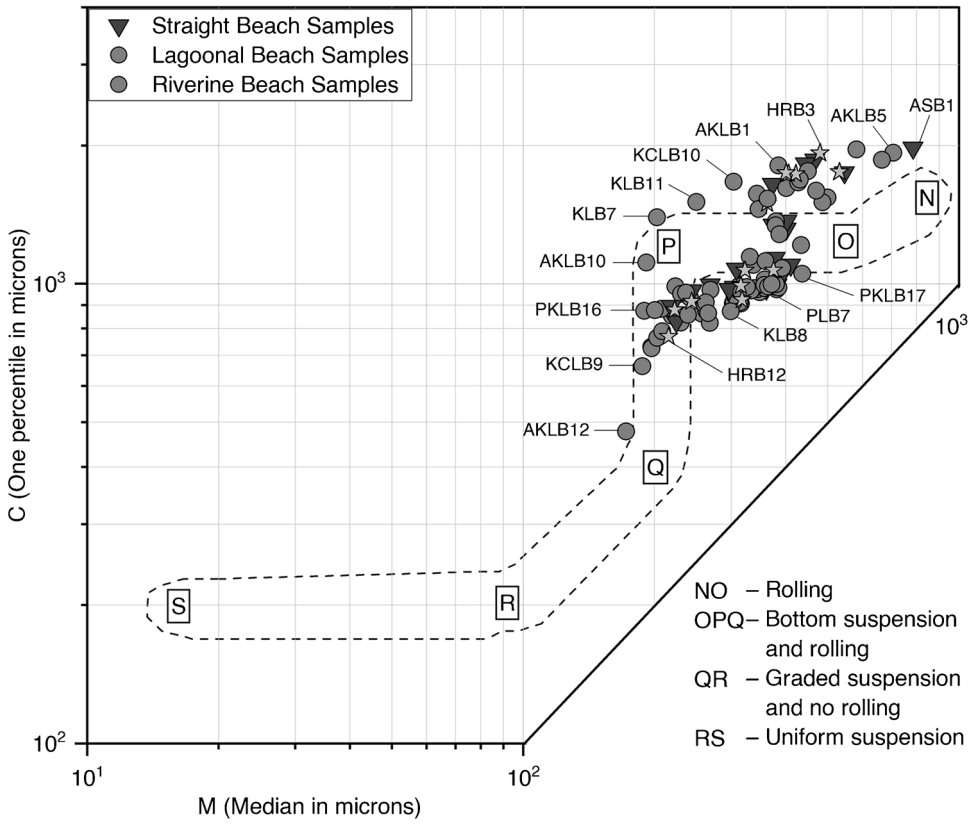

Fig. 7 The tractive current plot showing the mode of sediment transportation on the SE coast, Sri Lanka. This plot displays the rolling (NO), bottom suspension with rolling (OPQ), graded suspension (QR) and uniform suspension (RS)

Table 2 The quartz microtextures on lagoonal, riverine and direct beach deposits from SE coast, Sri Lanka. Vos et al. (2014) environmental discrimination scheme is added to construct the paleoenvironments of placers. Quantitative categories: abundant (*A*, > 75% of grains), common (*C*, 50–75%), sparse (*S*, 5–50%) and rare (*R*, < 5%)

Quartz microtextures		This study			Palaeoenvironment (Environmental discrimination by Vos et al. (2014))					
		Straight beach (siliciclastic)	Lagoonal beach (black placer)	Riverine beach (red placer)	Fluvial (low energy)	Fluvial (high energy)	Inter-tidal zone	Subtidal zone	Littoral dune	Alteration
Mechanical	Angular grains	-	-	-	C	S	-	S	-	-
	Subangular grains	S	C	S	C	C	C	C	C	-
	Subrounded or rounded grains	A	S	C	C	C	A	C	A	-
	Bulbous edges	S	S	S	-	-	-	-	A	-
	Medium conchoidal fractures (< 100 µm)	A	S	C	-	C	C	-	S	-
	Large conchoidal fracture (> 100 µm)	C	S	S	-	S	-	-	-	-
	Arcuate or straight steps	C	-	S	-	C	C	-	C	-
	Meandering ridges	S	S	S	-	-	-	-	C	-
	Graded arcs	C	S	S	-	S	S	-	C	C
	V-shaped percussion cracks	A	C	C	S	A	A	S	S	-
	Straight or curved grooves	C	S	-	-	C	A	S	S	-
	Upturned plates	S	S	S	-	S	S	-	A	-
	Crescentic percussion marks	S	S	S	-	S	S	-	C	-
	Parallel striations	-	-	-	-	-	-	-	-	-
Chemical	Oriented etch pits	-	-	-	-	-	C	A	-	C
	Solution pits	C	A	A	S	S	S	C	-	C
	Silica globules or flowers or pellicles	-	-	-	C	-	A	-	C	C
	Crystalline overgrowths	-	-	S	S	-	-	-	-	A
Combined	Low relief	-	S	S	-	C	-	-	A	C
	Medium relief	A	C	A	A	A	A	A	C	C
	High relief	-	S	S	-	C	-	-	-	-
	Elongated depressions	S	S	S	-	-	-	-	C	-
	Chattermarks	-	S	-	-	S	S	-	-	-
	Adhering particles	C	A	C	-	-	-	-	S	C
	Arcuate or circular cracks	S	-	C	-	-	-	-	-	C

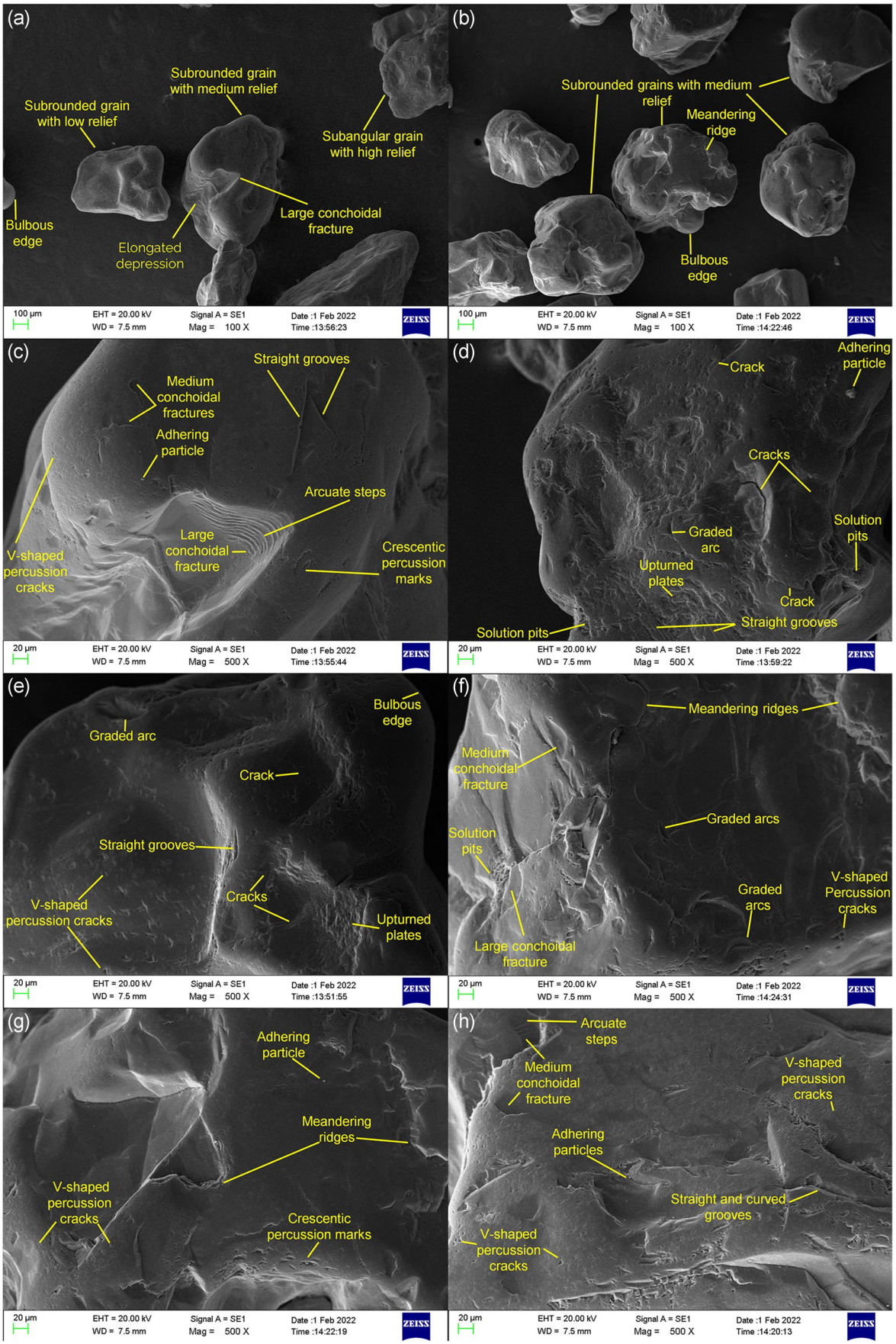
(a)
Subrounded grain with low relief
Subrounded grain with medium relief
Subangular grain with high relief
Bulbous edge
Elongated depression
Large conchoidal fracture
100 µm EHT = 20.00 kV WD = 7.5 mm Signal A = SE1 Mag = 100 X Date :1 Feb 2022 Time :13:56:23 ZEISS
(b)
Subrounded grains with medium relief
Meandering ridge
Bulbous edge
100 µm EHT = 20.00 kV WD = 7.5 mm Signal A = SE1 Mag = 100 X Date :1 Feb 2022 Time :14:22:46 ZEISS
(c)
Straight grooves
Medium conchoidal fractures
Adhering particle
Arcuate steps
V-shaped percussion cracks
Large conchoidal fracture
Crescentic percussion marks
20 µm EHT = 20.00 kV WD = 7.5 mm Signal A = SE1 Mag = 500 X Date :1 Feb 2022 Time :13:55:44 ZEISS
(d)
Crack
Adhering particle
Cracks
Graded arc
Solution pits
Upturned plates
Crack
Solution pits
Straight grooves
20 µm EHT = 20.00 kV WD = 7.5 mm Signal A = SE1 Mag = 500 X Date :1 Feb 2022 Time :13:59:22 ZEISS
(e)
Bulbous edge
Graded arc
Crack
Straight grooves
Cracks
V-shaped percussion cracks
Upturned plates
20 µm EHT = 20.00 kV WD = 7.5 mm Signal A = SE1 Mag = 500 X Date :1 Feb 2022 Time :13:51:55 ZEISS
(f)
Meandering ridges
Medium conchoidal fracture
Graded arcs
Solution pits
Graded arcs
V-shaped Percussion cracks
Large conchoidal fracture
20 µm EHT = 20.00 kV WD = 7.5 mm Signal A = SE1 Mag = 500 X Date :1 Feb 2022 Time :14:24:31 ZEISS
(g)
Adhering particle
Meandering ridges
V-shaped percussion cracks
Crescentic percussion marks
20 µm EHT = 20.00 kV WD = 7.5 mm Signal A = SE1 Mag = 500 X Date :1 Feb 2022 Time :14:22:19 ZEISS
(h)
Arcuate steps
Medium conchoidal fracture
V-shaped percussion cracks
Adhering particles
Straight and curved grooves
V-shaped percussion cracks
20 µm EHT = 20.00 kV WD = 7.5 mm Signal A = SE1 Mag = 500 X Date :1 Feb 2022 Time :14:20:13 ZEISS

◂ **Fig. 8** The quartz grain microphotographs of siliciclastic deposits in coastal environments. (**a**) Subrounded grain with medium relief, large conchoidal fracture and elongated depression; subrounded grain with low relief and bulbous edge; subangular grain with high relief; (**b**) subrounded grains with medium relief, meandering ridge and bulbous edge; (**c**) grain surface with medium conchoidal fractures, straight grooves, adhering particle, arcuate steps, large conchoidal fracture, *V*-shaped percussion cracks and crescentic percussion marks; (**d**) grain surface with upturned plates, solution pits, cracks, graded arc, adhering particle and straight grooves; (**e**) grain surface with upturned plates, bulbous edge, cracks, graded arc, straight grooves and *V*-shaped percussion cracks; (**f**) grain surface with medium conchoidal fractures, large conchoidal fracture, *V*-shaped percussion cracks, meandering ridges, graded arcs and solution pits; (**g**) grain surface with *V*-shaped percussion cracks, meandering ridges, adhering particle and crescentic percussion marks; (**h**) grain surface with *V*-shaped percussion cracks, medium conchoidal fractures, arcuate steps, adhering particles and straight and curved grooves

effective aeolian processes (Rajganapathi et al. 2013; Sinha et al. 2022; Tamura et al. 2018).

Sediment transportation dynamics

The tractive current pattern (TCP) of the CM plot has been used to distinguish sedimentary movements during coastal sediment deposition (Fig. 7) (Pradhan et al. 2020; Sinha et al. 2022). The value of *C* is sensitive to the capabilities of the transport agent (diameter of the coarsest 1% in cumulative size distribution). The value of *M* indicates the median sized sediment transport of the medium (Chima and Baiyegunhi 2022; Mout and Sarmah 2022). The TCP is divided into four parts, namely rolling (NO), bottom suspension with rolling (OPQ), graded suspension (QR) and uniform suspension (RS). The OP and PQ fields show high to low rolling modes in the OPQ segment.

The lagoonal, riverine and straight beach deposits are projected into the ON and OPQ fields, showing sedimentary movements rolling with bottom suspension (Fig. 7). There is no distinction between the coastal environments. The beach deposits occur in the OP field and indicate dominant rolling with bottom suspension movements. However, the coarse siliciclastic deposits in each environment fall in the NO field indicating the higher rolling sedimentary movements at high-energy wave actions (Passega 1964). The most uniform black and red placer deposits fall in the PQ field suggesting prevailed dominant bottom suspension with rolling movements at respectively lower energy actions (Passega 1964).

Microtextual attributes for transportation history

Totally, 25 mechanical and chemical microtextures are identified on the surface of the quartz grains (Table 2).

Paleoenvironment of siliciclastic deposits in straight coastal environment

The siliciclastic deposits exposed in straight beaches are composed of abundant subrounded quartz grains with medium relief (>75% of grains) and subangular quartz grains (50–5%, (Fig. 8a, b)). Conchoidal fractures (Fig. 8c, f, h) and *V*-shaped percussion cracks (Fig. 8e–h) are significant on their grain surfaces. Graded arcs (Fig. 8d–f), straight/curved grooves (Fig. 8c–e), solution pits (Fig. 8d, f) and adhering particles (Fig. 8g, h) are common on the sand grains. However, arcuate cracks (Fig. 8d, e), crescentic percussion marks (Fig. 8c, g), bulbous edges (Fig. 8a, b), meandering ridges (Fig. 8f, g), upturned plates (Fig. 8d, e) and elongated depressions (Fig. 8a) are sparse features.

Intense abrasions in the intertidal zone are attributed to the wearing of quartz grain boundaries to rounded in shape (Ramos-Vázquez and Armstrong-Altrin 2020; Silpa et al. 2016). Medium conchoidal fractures (Fig. 8c, f, h) and *V*-shaped percussion cracks (Fig. 8e–h) are indicative for the prevailed grain-to-grain impact during the high-energy littoral transport (Mahaney 2002; Ramos-Vázquez and Armstrong-Altrin 2021). Similarly, the fluvial processes is responsible in formation of these microtextures prior to being deposited on the beach faces (Ramos-Vázquez and Armstrong-Altrin 2020). Large conchoidal fractures with arcuate and straight steps evidenced for the crystalline rock sources and transportation through rivers (Fig. 8c, f, h (Armstrong-Altrin and Natalhy-Pineda 2014; Krishnan et al. 2015)). However, the conchoidal fractures are formed only on the grain surfaces that contain *V*-shaped percussion cracks (Fig. 8c, h) in high-energy coastal environments. Within the littoral zone, grooves are formed due to the movement of grains that energised by wave action (Armstrong-Altrin 2020; Silpa et al. 2016), while adhering particles are due to the grain collisions (Mejía-Ledezma et al. 2020). Although, the adhering particles in the siliciclastic have been largely eliminated during the sample preparation process. The graded arcs show strong collisions between grains, which occur in littoral dune environments (Vos et al. 2014). The solution pits are typically formed in relatively immobile sub-aqueous environments by dissolution or diagenetic processes (Li et al. 2020; Mejía-Ledezma et al. 2020).

In sub-aqueous conditions, crescentic percussion marks, bulbous edges, polished elongated depressions and meandering ridges occur during wind-driven transport, often indicating pre-aeolian sediments deposited in the intertidal zone while upturned plates are formed in the case of high-energy

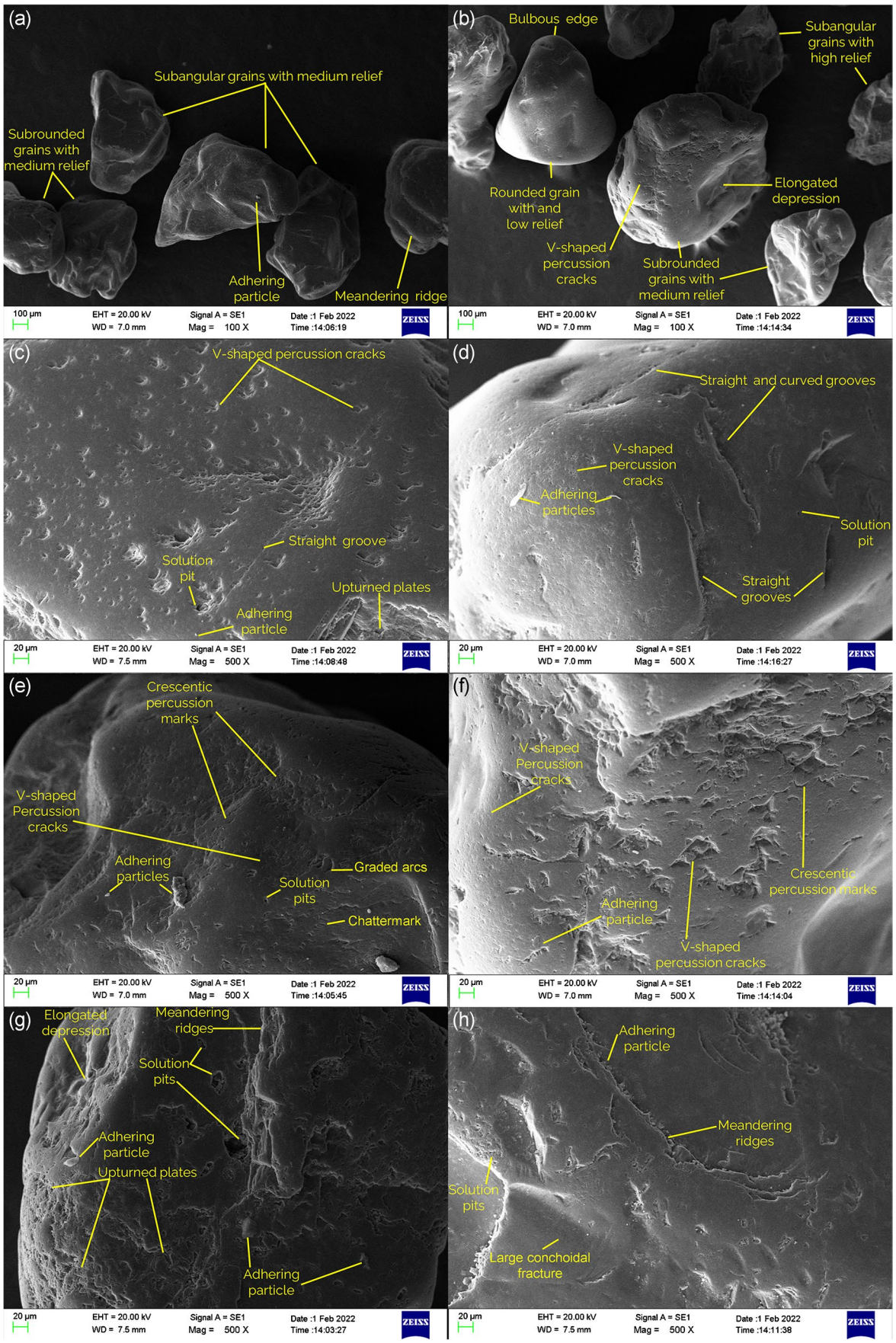
(a)
Subangular grains with medium relief
Subrounded grains with medium relief
Adhering particle
Meandering ridge
100 µm EHT = 20.00 kV WD = 7.0 mm Signal A = SE1 Mag = 100 X Date :1 Feb 2022 Time :14:06:19 ZEISS
(b)
Bulbous edge
Subangular grains with high relief
Rounded grain with and low relief
Elongated depression
V-shaped percussion cracks
Subrounded grains with medium relief
100 µm EHT = 20.00 kV WD = 7.0 mm Signal A = SE1 Mag = 100 X Date :1 Feb 2022 Time :14:14:34 ZEISS
(c)
V-shaped percussion cracks
Straight groove
Solution pit
Upturned plates
Adhering particle
20 µm EHT = 20.00 kV WD = 7.5 mm Signal A = SE1 Mag = 500 X Date :1 Feb 2022 Time :14:08:48 ZEISS
(d)
Straight and curved grooves
V-shaped percussion cracks
Adhering particles
Solution pit
Straight grooves
20 µm EHT = 20.00 kV WD = 7.0 mm Signal A = SE1 Mag = 500 X Date :1 Feb 2022 Time :14:16:27 ZEISS
(e)
Crescentic percussion marks
V-shaped Percussion cracks
Adhering particles
Graded arcs
Solution pits
Chattermark
20 µm EHT = 20.00 kV WD = 7.0 mm Signal A = SE1 Mag = 500 X Date :1 Feb 2022 Time :14:05:45 ZEISS
(f)
V-shaped Percussion cracks
Crescentic percussion marks
Adhering particle
V-shaped percussion cracks
20 µm EHT = 20.00 kV WD = 7.0 mm Signal A = SE1 Mag = 500 X Date :1 Feb 2022 Time :14:14:04 ZEISS
(g)
Elongated depression
Meandering ridges
Solution pits
Adhering particle
Upturned plates
Adhering particle
20 µm EHT = 20.00 kV WD = 7.5 mm Signal A = SE1 Mag = 500 X Date :1 Feb 2022 Time :14:03:27 ZEISS
(h)
Adhering particle
Meandering ridges
Solution pits
Large conchoidal fracture
20 µm EHT = 20.00 kV WD = 7.5 mm Signal A = SE1 Mag = 500 X Date :1 Feb 2022 Time :14:11:38 ZEISS

◂ **Fig. 9** The quartz grain microphotographs of black heavy placer deposits in lagoonal beach environments. (**a**) Subrounded grains with medium relief; subangular grains with medium relief, adhering particle and meandering ridge; (**b**) rounded grain with low relief and bulbous edge; subrounded grains with medium relief, *V*-shaped percussion cracks and elongated depression; subangular grains with high relief; (**c**) grain surface with *V*-shaped percussion cracks, straight groove, upturned plates, adhering particle and solution pit; (**d**) grain surface with solution pit, adhering particles, *V*-shaped percussion cracks and straight or curved grooves; (**e**) grain surface with crescentic percussion marks, graded arcs, solution pits, adhering particles, chattermark and *V*-shaped percussion cracks; (**f**) grain surface with crescentic percussion marks, *V*-shaped percussion cracks and adhering particle; (**g**) grain surface with meandering ridges, adhering particles, elongated depression, solution pits and upturned plates; (**h**) grain surface with solution pits, large conchoidal fracture, adhering particles and meandering ridges

aeolian collisions of cleavage planes (Costa et al. 2013; Z. Li et al. 2020; Mahaney 2002; Udayaganesan et al. 2011; Vos et al. 2014). However, such microtextures are sparse in these sediments. The post-chemical alteration processes diplay a number of cracks and solution pits (Fig. 8d–e, (Armstrong-Altrin and Natalhy-Pineda 2014; Gandhi et al. 2008)).

The siliciclastic along the straight beaches reveals the specific microtextures indicating the different sedimentary cycles: (i) sub-aqueous beach processes (subrounded grains, *V*-shaped percussion cracks, medium relief, large conchoidal fracture and straight or curved grooves), (ii) fluvial processes (large conchoidal fracture and *V*-shaped percussion cracks), (iii) aeolian processes (upturned plates, crescentic percussion marks, bulbous edges, polished elongated depressions and meandering ridges) and (iv) chemical alteration processes (cracks and solution pits). The crosscutting relationships between environment specific microtextures advocate precise timescale of these sedimentation episodes (Mejía-Ledezma et al. 2020; Sweet and Soreghan 2010). It is evident that the siliciclastic deposits are primarily and subsequently controlled by high-energy sub-aqueous beach processes with sparse aeolian process and affirm that these quartz grains are of crystalline rock sources. Due to the inter tidal, aeolian grain abrasions and source-sink distances, the fluvial evidence of these grains may not be possible to preserve.

Paleoenvironment of black-coloured placer in lagoonal beach environment

The microtextures of quartz grains in placer are characterised by abundant solution pits and adhering particles inferring the processes of immobile subtidal zones (Fig. 9g, h, (Vos et al. 2014). The solution pits within chemically altered irregular cavities are larger than 20 µm (Fig. 9g). The subangular grains (Fig. 9a, b), *V*-shaped percussion cracks (Fig. 9c, d, f) and medium relief (Fig. 9a, b) are common. These microtextures are caused by both beach and fluvial processes (Itamiya et al. 2019; Krishnan et al. 2015). Specially, some grains show *V*-shaped percussion cracks larger than 20 µm in diameter that may indicate high-energy grain-to-grain impacts in sub-aqueous environment (Fig. 9c, f, (Armstrong-Altrin and Natalhy-Pineda 2014; Vos et al. 2014)). However, subrounded grains (Fig. 9a, b), conchoidal fractures (Fig. 9h) and straight or curved grooves (Fig. 9c, d) are indicating prevailed less sub-aqueous beach processes compared to siliciclastic deposits. Therefore, the relative grain angularity of these sediments indicates short source-sinking distances derived from fluvial environments (Armstrong-Altrin and Natalhy-Pineda 2014; Hossain et al. 2014). Similarly, bulbous edges (Fig. 9b), meandering ridges (Fig. 9g, h), graded arcs (Fig. 9e), upturned plates (Fig. 9c, g), crescentic percussion marks (Fig. 9e, f) and elongated depressions (Fig. 9b, g) are sparse and unique to terrestrial transport processes (J. Li et al. 2021; Li et al. 2020; Vos et al. 2014). Chatter marks (Fig. 9e) are unique microtextures for the glacial environment (Peterknecht and Tietz 2011; Ramos-Vázquez and Armstrong-Altrin 2020). However, being far away from such environments, this sparse microtexture attributed for tropical climatic conditions and high-energy sub-aqueous environment (Armstrong-Altrin and Natalhy-Pineda 2014; Mohammad et al. 2020). In addition, low relief-rounded grains and high relief subangular grains indicate inputs from aeolian and fluvial cycles (Sweet and Soreghan 2010). With reference to varied sedimentary cycles, *V*-shape and crescentic percussion marks on the same grain surfaces, indicating aeolian contributions to swash deposits (Fig. 9e, f). Furthermore, chemically altered upturned plates with elongated depressions indicate pre-aeolian processes (Fig. 9g). The crystalline rock sources of quartz in black placer are relatively closer compared to siliciclastic. Furthermore, these placer deposits are characterised by higher fluvial, chemical alteration processes and low sub-aqueous beach processes.

Paleoenvironment of red-coloured placer in riverine beach environment

The red placer deposits in the riverine beach are characterised by solution pits (Fig. 10d, f, g) and medium relief (Fig. 10a, b). Besides, arcuate or circular cracks (Fig. 10c, d, f) are common with lesser crystalline growths (Fig. 10c) inferring the chemical alteration processes. Strikingly, circular cracks occur with depressions indicating high impact on the grain surface (Fig. 10c, (Gandhi et al. 2008)). Rarely occurring crystalline

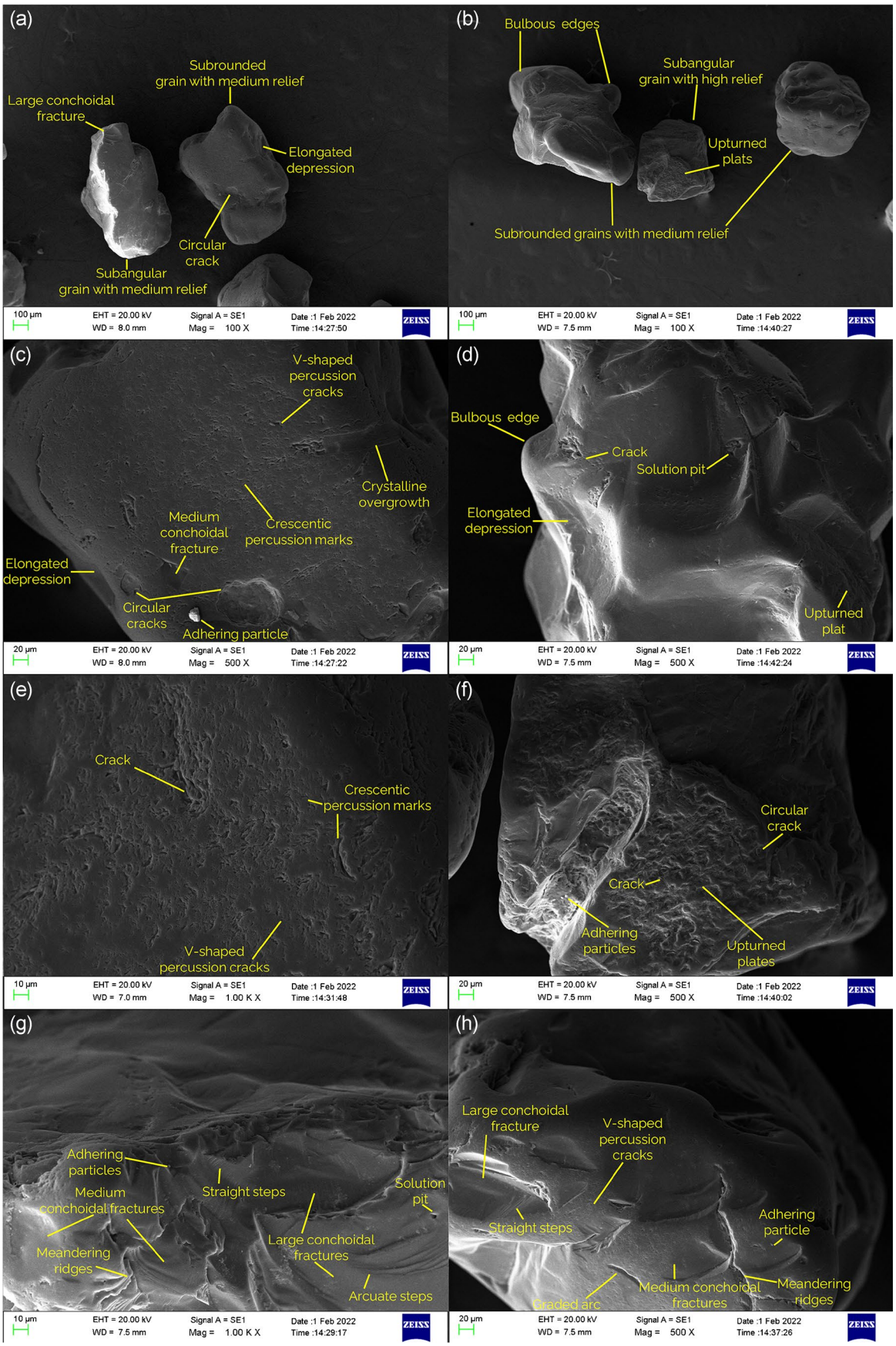
(a)
Subrounded grain with medium relief
Large conchoidal fracture
Elongated depression
Circular crack
Subangular grain with medium relief
100 µm EHT = 20.00 kV WD = 8.0 mm Signal A = SE1 Mag = 100 X Date :1 Feb 2022 Time :14:27:50 ZEISS
(b)
Bulbous edges
Subangular grain with high relief
Upturned plats
Subrounded grains with medium relief
100 µm EHT = 20.00 kV WD = 7.5 mm Signal A = SE1 Mag = 100 X Date :1 Feb 2022 Time :14:40:27 ZEISS
(c)
V-shaped percussion cracks
Crystalline overgrowth
Medium conchoidal fracture
Crescentic percussion marks
Elongated depression
Circular cracks
Adhering particle
20 µm EHT = 20.00 kV WD = 8.0 mm Signal A = SE1 Mag = 500 X Date :1 Feb 2022 Time :14:27:22 ZEISS
(d)
Bulbous edge
Crack
Solution pit
Elongated depression
Upturned plat
20 µm EHT = 20.00 kV WD = 7.5 mm Signal A = SE1 Mag = 500 X Date :1 Feb 2022 Time :14:42:24 ZEISS
(e)
Crack
Crescentic percussion marks
V-shaped percussion cracks
10 µm EHT = 20.00 kV WD = 7.0 mm Signal A = SE1 Mag = 1.00 K X Date :1 Feb 2022 Time :14:31:48 ZEISS
(f)
Circular crack
Crack
Adhering particles
Upturned plates
20 µm EHT = 20.00 kV WD = 7.5 mm Signal A = SE1 Mag = 500 X Date :1 Feb 2022 Time :14:40:02 ZEISS
(g)
Adhering particles
Medium conchoidal fractures
Straight steps
Solution pit
Meandering ridges
Large conchoidal fractures
Arcuate steps
10 µm EHT = 20.00 kV WD = 7.5 mm Signal A = SE1 Mag = 1.00 K X Date :1 Feb 2022 Time :14:29:17 ZEISS
(h)
Large conchoidal fracture
V-shaped percussion cracks
Straight steps
Adhering particle
Graded arc
Medium conchoidal fractures
Meandering ridges
20 µm EHT = 20.00 kV WD = 7.5 mm Signal A = SE1 Mag = 500 X Date :1 Feb 2022 Time :14:37:26 ZEISS

◂ **Fig. 10** The quartz grain microphotographs of red heavy placer deposits in riverine beach environment. (**a**) Subrounded grain with medium relief, circular crack and elongated depression; subangular grain with medium relief and large conchoidal fracture; (**b**) subrounded grains with medium relief and bulbous edges; subangular grain with high relief and upturned plats; (**c**) grain surface with medium conchoidal fracture, adhering particle, *V*-shaped percussion cracks, elongated depression, circular cracks, crystalline overgrowth and crescentic percussion marks; (**d**) grain surface with upturned plates, solution pits, cracks, bulbous edges and elongated depression; (**e**) grain surface with crack, crescentic percussion marks and *V*-shaped percussion cracks; (**f**) grain surface with crack, circular cracks, upturned plates and adhering particles; (**g**) grain surface with meandering ridges, adhering particle, medium conchoidal fractures, large conchoidal fractures, straight steps, arcuate steps and solution pit; (**h**) grain surface with *V*-shaped percussion cracks, medium conchoidal fractures, large conchoidal fractures, straight steps, adhering particle, meandering ridges and graded arc

overgrowth crosscut a chemically modified surface and develop as a filler surface (Fig. 10c). Chemically alternated microtextures in red placer deposits indicate for diagenetic processes in subtropical regions (Sweet and Soreghan 2010; Vos et al. 2014). Also, quartz grains from these deposits commonly show subrounded shapes (Fig. 10a, b), medium conchoidal fractures (Fig. 10g, h), *V*-shaped percussion cracks (Fig. 10c, e, h) and adhering particles (Fig. 10c, g). These microtextures are evident for prevailed grain-grain impacts and abrasive processes in the beach or fluvial environment (Itamiya et al. 2019; Krishnan et al. 2015). Subangular grains (Fig. 10a, b), large conchoidal fracture (Fig. 10g, h) and arcuate or straight steps (Fig. 10g, h) are sparse. Similar to siliciclastic deposits, large conchoidal fractures occur as crosscutting surfaces that contain *V*-shaped percussion cracks (Fig. 10h). This crosscutting microtexture interprets that higher energy grain impacts are more related to the coastal environment than to the fluvial environment. Similar to the other deposits, bulbous edges (Fig. 10b), meandering ridges (Fig. 10g, h), graded arcs (Fig. 10h), upturned plates (Fig. 10d, f), crescentic percussion marks (Fig. 10c, e), low relief, high relief (Fig. 10b) and elongated depressions (Fig. 10a, d) are sparse and indicate low contribution of aeolian processes to coastal deposits. All overprinted microtextures occur on other deposits are similar and indicate the pre-aeolian processes in red placers (Fig. 10c–f). Therefore, aeolian sedimentation has a similar influence on the siliciclastic, black and red placers. It can be confirmed that crystalline rock sources of quartz in red heavy placer deposits have moderate distances compared to the black placers. Furthermore, these placer deposits are characterised by chemical alteration processes and moderate sub-aqueous beach processes.

Conclusions

This study revealed the presence of black and red heavy placer deposits along the lagoonal and riverine beaches of SE coast of Sri Lanka respectively. These placer deposits are related to coarse-skewed leptokurtic to platykurtic fine sand size distributions whereas the non-placer siliciclastic beach deposits are abundant medium grains. The black placer deposits are ilmenite rich titanium placers with high uniformity fine sands. The red placers are almandine placers mixed with titanium mineral placers and show medium to fine sand mixtures. During the deposition, placer sediments may have been transported through dominant bottom suspension with rolling sedimentary movements compared to the siliciclastic deposits with higher rolling dynamics. The weak wave-generated processes and higher settling capacity of sediments may control the settlement of heavy placer deposits on swash zone with scattered distributions.

The sediments from straight, lagoonal and riverine beach environments display a total of 25 types of microtextures indicating the influence from sub-aqueous-beach, fluvial, aeolian and chemical alteration processes. With the order of siliciclastic, red to black placer deposits, the sediments show decrease in source-sinking distances, decreases in sub-aqueous beach processes and increase in fluvial processes. Chemical alteration processes are higher in the heavy placer deposits attributing to the deposition in an immobile low energy environment. Both types of heavy mineral placers may have been derived from metamorphic rocks of the Vijayan Complex and Highland-Vijayan tectonic mixed zone. Furthermore, a seasonal variation study is recommended as a forward research for identifying the vertical extensions and economic potential of mineralised zones in river and lagoon related beaches.

Acknowledgements Authors are thankful for excellent field assistance from Y.M.S.G. Imantha, U.D.C. Wickramarathna, A.G.A.L. Danushka, P.M.I.U. Aththanayaka and S.S.S.T. Fernando.

Author contribution Chaturanga Sandaruwan: conceptualization, methodology, software, formal analysis, data curation, writing—original draft. Nadeesha Madugalla: conceptualization, validation, resources, writing—review and editing, supervision. Madurya Adikaram: conceptualization, validation, resources, writing—review and editing, supervision. Amarasooriya Pitawala: conceptualization, resources, writing—review and editing, supervision. Tharanga Udagedara: investigation, resources, formal analysis, data curation.

Funding This study is financially supported by the South Eastern University of Sri Lanka (SEUSL) through the grant No. SEU/ASA/RG/2021/05, and it is greatly acknowledged.

Data Availability The data that supports the findings of this study are available on request from the corresponding author.

Declarations

Conflict of interest The authors declare that they have no competing interests.

References

Amalan K, Ratnayake AS, Ratnayake NP, Weththasinghe SM, Dushyantha N, Lakmali N, Premasiri R (2018) Influence of nearshore sediment dynamics on the distribution of heavy mineral placer deposits in Sri Lanka. Environ Earth Sci 77:1–13. https://doi.org/10.1007/s12665-018-7914-4

Arachchi MK, Dharmapriya PL, Malaviarachchi SPK, Samaranayake SA, Subasinghe ND (2017) Petrological characteristics of post-tectonic intrusive dolerites and gabbros in the Vijayan Complex, Sri Lanka. J Geol Soc Sri Lanka 18:89–99

Armstrong-Altrin JS (2020) Detrital zircon U-Pb geochronology and geochemistry of the Riachuelos and Palma Sola beach sediments, Veracruz State, Gulf of Mexico: a new insight on palaeoenvironment. J Palaeogeogr 9:1–27. https://doi.org/10.1186/s42501-020-00075-9

Armstrong-Altrin JS, Natalhy-Pineda O (2014) Microtextures of detrital sand grains from the Tecolutla, Nautla, and Veracruz beaches, western Gulf of Mexico, Mexico: implications for depositional environment and paleoclimate. Arab J Geosci 7:4321–4333. https://doi.org/10.1007/s12517-013-1088-x

Azidane H, Michel B, Bouhaddioui MEl, Haddout S, Magrane B, Benmohammadi A, (2021) Grain size analysis and characterization of sedimentary environment along the Atlantic Coast, Kenitra (Morocco). Mar Georesour Geotechnol 39:569–576. https://doi.org/10.1080/1064119X.2020.1726536

Best ME (2015) Mineral resources. In: Schubert G (ed) Treatise on geophysics, 2nd edn. Elsevier, Amsterdam, pp 525–556. https://doi.org/10.1016/B978-0-444-53802-4.00200-1

Biederman EW (1962) Distinction of shoreline environments in New Jersey. J Sediment Res 32:181–200. https://doi.org/10.1306/74D70C72-2B21-11D7-8648000102C1865D

Blott SJ, Pye K (2001) Gradistat: A grain size distribution and statistics package for the analysis of unconsolidated sediments. Earth Surf Proc Land 26:1237–1248. https://doi.org/10.1002/esp.261

Bujan N, Cox R, Masselink G (2019) From fine sand to boulders: examining the relationship between beach-face slope and sediment size. Mar Geol 417:106012. https://doi.org/10.1016/j.margeo.2019.106012

Cardona JPM, Mas JMG, Bellón AS, Domínguez-Bella S, López JM (2005) Surface textures of heavy-mineral grains: a new contribution to provenance studies. Sed Geol 174:223–235. https://doi.org/10.1016/j.sedgeo.2004.12.006

Cheepurupalli NR, Radha BA, Reddy KSN, Dhanamjayarao EN, Dayal AM (2012) Heavy Mineral distribution studies in different micro-environments of Bhimunipatnam coast, Andhra Pradesh, India. Int J Sci Res Publ 2:1–10

Chima P, Baiyegunhi C (2022) Textural characteristics, mode of transportation and depositional environment of the Stormberg Group in the Eastern Cape, South Africa: evidence from grain size and lithofacies analyses. Geologos 28:61–78. https://doi.org/10.1515/geo-2020-0135

Cooray PG (1984) An introduction to the geology of Sri Lanka (Ceylon). National Museums of Sri Lanka Publication, Colombo

Cooray PG (1994) The precambrian of Sri Lanka: a historical review. Precambr Res 66:3–18. https://doi.org/10.1016/0301-9268(94)90041-8

Cooray PG, Katupotha J (1991) Geological Evolution of the coastal zone of Sri Lanka, Proceedings of the Symposium on "Causes of Coastal Erosion in Sri Lanka". Colombo, Sri Lanka, pp 5–26. https://doi.org/10.13140/RG.2.1.1278.2566

Costa PJM, Andrade C, Mahaney WC, Marques F, Freire P, Freitas MC, Janardo C, Oliveira MA, Silva T, Lopes V (2013) Geomorphology Aeolian microtextures in silica spheres induced in a wind tunnel experiment : comparison with aeolian quartz. Geomorphology 180:120–129. https://doi.org/10.1016/j.geomorph.2012.09.011

Elsherif EA, Badawi A, Abdelkader T (2020) Grain size distribution and environmental implications of rosetta beach, mediterranean sea coast, Egypt. Egypt J Aquat Biol Fish 24:349–370. https://doi.org/10.21608/EJABF.2020.70860

Folk RL, Ward WC (1957) Brazos river bar [Texas]; a study in the significance of grain size parameters. J Sediment Res 27:3–26. https://doi.org/10.1306/74D70646-2B21-11D7-8648000102C1865D

Gandhi MS, Solai A, Chandrasekaran K, Rammohan V (2008) Sediment characteristics and heavy mineral distribution in tamiraparani estuary and off Tuticorin, Tamil Nadu-SEM Studies. J Earth Sci India 1:102–118 http://www.earthscienceindia.info/. Accessed 02 March 2022

Haldar SK, Tišljar J (2014) Mineral deposits: host rocks and origin. In: Haldar SK, Tišljar J (eds) Introduction to mineralogy and petrology. Elsevier, Amsterdam, pp 261–279. https://doi.org/10.1016/B978-0-12-408133-8.00008-0

Haldar SK (2013) Economic mineral deposits and host rocks. In: Haldar SK (ed) Mineral exploration. Elsevier, pp 23–39. https://doi.org/10.1016/B978-0-12-416005-7.00002-7

He XF, Santosh M, Tsunogae T, Malaviarachchi SPK, Dharmapriya PL (2016) Neoproterozoic arc accretion along the "eastern suture" in Sri Lanka during Gondwana assembly. Precambr Res 279:57–80. https://doi.org/10.1016/j.precamres.2016.04.006

Hoshino M, Sanematsu K, Watanabe Y (2016) REE mineralogy and resources. In: Bünzli JC, Pecharsky VK (eds) Handbook on the physics and chemistry of rare earths. Elsevier, Amsterdam, pp 129–291. https://doi.org/10.1016/BS.HPCRE.2016.03.006

Hossain HMZ, Tarek M, Armstrong-Altrin JS, Monir MMU, Ahmed MT, Ahmed SI, Hernandez-Coronado CJ (2014) Microtextures of detrital sand grains from the Cox's Bazar beach, Bangladesh: implications for provenance and depositional environment. Carpathian J Earth Environ Sci 9:187–197

Hossain HMZ, Armstrong-Altrin JS, Jamil AHMN, Rahman MM, Hernández-Coronado CJ, Ramos-Vázquez MA (2020) Microtextures on quartz grains in the Kuakata beach, Bangladesh: implications for provenance and depositional environment. Arab J Geosci 13:1–12. https://doi.org/10.1007/s12517-020-5265-4

Inman DL (1949) Sorting of sediments in the light of fluid mechanics. SEPM J Sediment Res 19:51–70. https://doi.org/10.1306/d426934b-2b26-11d7-8648000102c1865d

Itamiya H, Sugita R, Sugai T (2019) Analysis of the surface microtextures and morphologies of beach quartz grains in Japan and implications for provenance research. Prog Earth Planet Sci 6:1–14. https://doi.org/10.1186/s40645-019-0287-9

Jiang C, Wu Z, Chen J, Deng B, Long Y (2015) Sorting and sedimentology character of sandy beach under wave action. Proc Eng 116:771–777. https://doi.org/10.1016/j.proeng.2015.08.363

Jinadasa SUP, Wijayadeva A (2013) Geological approach for placer mineral exploration in Eastern coast of Sri Lanka - a case study. J Natl Aquat Resourc Res Dev Agency 42:73–79

Katupotha J, Gamage S (2020) Understanding the river basin classification of Sri Lanka. Wildlanka 8:175–197

Kehelpannala KVW (1997) Deformation of a high-grade Gondwana fragment, Sri Lanka. Gondwana Res 1:47–68. https://doi.org/10.1016/s1342-937x(05)70005-8

Krishnan NG, Nagendra R, Elango L (2015) Quartz surface microtextural studies of Cauvery River sediments, Tamil Nadu, India. Arab J Geosci 8:10665–10673. https://doi.org/10.1007/s12517-015-1995-0

Li Z, Yu X, Dong S, Chen Q, Zhang C (2020) Microtextural features on quartz grains from eolian sands in a subaqueous sedimentary environment : a case study in the hinterland of the Badain Jaran Desert, Northwest China. Aeolian Res 43:100573. https://doi.org/10.1016/j.aeolia.2020.100573

Li J, Wang X, Wu W (2021) Quantification of SEM quartz grain identifying the depositional environment. Arab J Geosci 14:1–11. https://doi.org/10.1007/s12517-021-07442-3

Mahaney WC, Stewart A, Kalm V (2001) Quantification of SEM microtextures useful in sedimentary environmental discrimination. Boreas 30:165–171. https://doi.org/10.1111/J.1502-3885.2001.TB01220.X

Mahaney WC (2002) Atlas of sand grain surface textures and applications. Oxford University Press, Oxford. https://books.google.com/books?hl=en&lr=&id=TQcv-Mby3NwC&oi=fnd&pg=PA3&dq=Mahaney,+W.C.,+2002.+Atlas+of+sand+grain+surface+textures+and+applications.&ots=tIRb15ARLZ&sig=FnoIwN4TG99nNGqXMXiet8Badnk. Accessed 19 May 2022

Manjula HAKL, Marambe MKAYA, Madugalla TBNS (2020) Economic appraisal of iron ore deposit in Buttala, Sri Lanka: preliminary mineral and chemical evidences. J Geol Soc Sri Lanka 21:47–55. https://doi.org/10.4038/jgssl.v21i1.37

Mathavan V, Dissanayake CB (1977) Garnets of Sri Lanka: their potential as abrasives. Wear 45:383–389

Mejía-Ledezma RO, Kasper-Zubillaga JJ, Alvarez-Sánchez LF, Mendieta-Lora M, Arellano-Torres E, Tetlalmatzi-Martínez JL, Gonzalez-Bermúdez A, Patiño-Andrade D, Armstrong-Altring JS (2020) Surface textures of quartz and ilmenite grains from dune and beach sands of the Gulf of Mexico Coast, Mexico: implications for fluvial, aeolian and marine transport. Aeol Res 45:100611. https://doi.org/10.1016/j.aeolia.2020.100611

Milisenda CC, Liew TC, Hofmann AW, Kroner A (1988) Isotopic mapping of age provinces in Precambrian high-grade terrains: Sri Lanka. J Geol 96:608–615. https://doi.org/10.1086/629256

Mohammad A, Bhanu Murthy P, Dhanamjaya Rao EN, Prasad H (2020) A study on textural characteristics, heavy mineral distribution and grain-microtextures of recent sediment in the coastal area between the Sarada and Gosthani rivers, east coast of India. Int J Sedim Res 35:484–503. https://doi.org/10.1016/j.ijsrc.2020.03.007

Mout JM, Sarmah RK (2022) Unraveling depositional mode and provenance of Kopili Formation, Northeast India. J Geol Soc India 98:496–504. https://doi.org/10.1007/s12594-022-2007-0

Naidu B, Sekhar R, Rao G, Krishna M (2016) Grain size distribution of coastal sands between Gosthani and Champavathi Rivers Confluence, East Coast of India. Andhra Pradesh J Ind Geophys Union 20:351–361

Narvekar J, Kumar SP (2006) Seasonal variability of the mixed layer in the central Bay of Bengal and associated changes in nutrients and chlorophyll. Deep Sea Res Part 1 Oceanogr Res Pap 53:820–835. https://doi.org/10.1016/j.dsr.2006.01.012

Ng SWP, Whitehouse MJ, Tam TPY, Jayasingha P, Wong JPM, Denyszyn SW, Yiu JSY, Chang SC (2017) Ca. 820–640 Ma SIMS U-Pb age signal in the peripheral Vijayan Complex, Sri Lanka: identifying magmatic pulses in the assembly of Gondwana. Precambr Res 294:244–256. https://doi.org/10.1016/j.precamres.2017.03.013

Palleyi S, Banoo S, Kar RN, Panda CR (2015) Textural and geochemical characteristics of off shore sediment of North Bay of Bengal: a statistical approach for marine metal pollution. Int J Sediment Res 30:208–222. https://doi.org/10.1016/j.ijsrc.2014.09.001

Passega R (1964) Grain size representation by CM patterns as a geologic tool. J Sediment Petrol 34:830–847. https://doi.org/10.1306/74d711a4-2b21-11d7-8648000102c1865d

Peterknecht KM, Tietz GF (2011) Chattermark trails: surface features on detrital quartz grains indicative of a tropical climate. J Sediment Res 81:153–158. https://doi.org/10.2110/jsr.2011.9

Pradhan UK, Sahoo RK, Pradhan S, Mohany PK, Mishra P (2020) Textural analysis of coastal sediments along East Coast of India. J Geol Soc India 95:67–74. https://doi.org/10.1007/s12594-020-1387-2

Rajapaksha AU, Vithanage M, Oze C, Bandara WMAT, Weerasooriya R (2012) Nickel and manganese release in serpentine soil from the Ussangoda Ultramafic Complex, Sri Lanka. Geoderma 189:1–9. https://doi.org/10.1016/j.geoderma.2012.04.019

Rajganapathi VC, Jitheshkumar N, Sundararajan M, Bhat KH, Velusamy S (2013) Grain size analysis and characterization of sedimentary environment along Thiruchendur coast, Tamilnadu, India. Arab J Geosci 6:4717–4728. https://doi.org/10.1007/s12517-012-0709-0

Rajmohan S, Hishamundavalens VS, Claude N (2016) Textural analysis and heavy mineral distribution studies of coastal sediments from Portonova to Gadilam River, along the east coast of Tamil Nadu. Int J Geol Earth Sci 2:33–42. https://doi.org/10.5281/ZENODO.1536875

Ramos-Vázquez MA, Armstrong-Altrin JS (2020) Provenance and palaeoenvironmental significance of microtextures in quartz and zircon grains from the Paseo del Mar and Bosque beaches, Gulf of Mexico. J Earth Syst Sci 129:1–16. https://doi.org/10.1007/s12040-020-01491-0

Ramos-Vázquez MA, Armstrong-Altrin JS (2021) Provenance of sediments from Barra del Tordo and Tesoro beaches, Tamaulipas State, northwestern Gulf of Mexico. J Palaeogeogr 10:1–17. https://doi.org/10.1186/s42501-021-00101-4

Rao BK, Ramaiah JS, Murthy PB, Swamy ASR (1993) Studies on heavy minerals in the Krishna river basin. J Indian Assoc Sediment 12:79–88

Richmond BM, Jaffe BE, Gelfenbaum G, Morton RA (2006) Geologic impacts of the 2004 Indian ocean tsunami on Indonesia, Sri Lanka, and the Maldives. Zeitschrift Fur Geomorphol Supplementband 146:235–251

Rosas J, Lopez O, Missimer TM, Coulibaly KM, Dehwah AHA, Sesler K, Lujan LR, Mantilla D (2014) Determination of hydraulic conductivity from grain-size distribution for different depositional environments. Groundwater 52:399–413. https://doi.org/10.1111/gwat.12078

Sandaruwan C, Adikaram M, Madugalla N, Pitawala A, Ishiga H, Udagedara T (2022) Mineralogy and geochemistry of beach sediments associated with the Precambrian crystalline rocks (Vijayan Complex) of Sri Lanka; perspective for heavy minerals. Reg Stud Mar Sci 55. https://doi.org/10.1016/j.rsma.2022.102579

Satyanarayana B, Van der Stocken T, Rans G, Kodikara KAS, Ronsmans G, Jayatissa LP, Husain ML, Koedam N, Dahdouh-Guebas F (2017) Island-wide coastal vulnerability assessment of Sri Lanka reveals that sand dunes, planted trees and natural vegetation may play a role as potential barriers against ocean surges. Global Ecol Conserv 12:144–157. https://doi.org/10.1016/j.gecco.2017.10.001

Silpa B, Srinivas R, Likhil A, Aneesh T, Prasad K, Sajan K (2016) Microtextures on quartz grains in the beach sediments of a high energy regime, Kerala, Southwest coast of India. Indian J Geo-Mar Sci (IJMS) 45:191–196

Silva EIL, Katupotha J, Amarasinghe O, Manthrithilake H, Ariyaratna R (2013) Lagoons of Sri Lanka: from the origins to the present. Colombo, Sri Lanka: International Water Management Institute(IWMI). https://doi.org/10.5337/2013.215

Sinha S, Mondal SK, Mondal S, Hansda S, Patra UK (2022) Deciphering grain size populations and hydromorphological characteristics of the beach-dune system of East Coast of India: implications to coastal resilience and hazard mitigation. Environ Earth Sci 81:20. https://doi.org/10.1007/s12665-022-10276-1

Subasinghe HCS, Ratnayake AS, Sameera KAG (2021) State-of-the-art and perspectives in the heavy mineral industry of Sri Lanka. Miner Econ 34:427–439. https://doi.org/10.1007/s13563-021-00274-3

Sweet DE, Soreghan GS (2010) Application of quartz sand microtextural analysis to infer cold-climate weathering for the equatorial fountain formation (Pennsylvanian-Permian, Colorado, U.S.A.). J Sediment Res 80:666–677. https://doi.org/10.2110/jsr.2010.061

Tamura T, Nicholas WA, Oliver TS, Brooke BP (2018) Coarse-sand beach ridges at Cowley Beach, north-eastern Australia: their formative processes and potential as records of tropical cyclone history. Sedimentology 65:721–744. https://doi.org/10.1111/ijlh.12426

Trenhaile AS (2005) Beach sediment characteristics. In: Schwartz ML (ed) Encyclopedia of Coastal Science. Springer, Netherlands, pp 177–179. https://doi.org/10.1007/1-4020-3880-1_41

Udayaganesan P, Angusamy N, Gujar AR, Rajamanickam GV (2011) Surface microtextures of quartz grains from the central coast of Tamil Nadu. J Geol Soc India 77:26–34

Van-Gosen BS, Fey DL, Shah AK, Verplanck PL, Hoefen TM (2014) Deposit model for heavy-mineral sands in coastal environments: U.S. Geological Survey Scientific Investigations Report 2010–5070–L. https://doi.org/10.3133/sir20105070L

Vos K, Vandenberghe N, Elsen J (2014) Surface textural analysis of quartz grains by scanning electron microscopy (SEM): from sample preparation to environmental interpretation. Earth Sci Rev 128:93–104. https://doi.org/10.1016/j.earscirev.2013.10.013

Wang P, Li Q, Li CF (2014) Hydrocarbon and mineral resources. In: Wang P, Li Q, Li CF (eds) Developments in marine geology. Elsevier, Amsterdam, pp 571–641. https://doi.org/10.1016/B978-0-444-59388-7.00007-X

Weerakkody U (1985) Geomorphological evolution of the southeastern coast of Sri Lanka. Thesis, University of Ruhuna. http://192.248.48.160/handle/iruor/778. Accessed 10 June 2022

Authors and Affiliations

Chaturanga Sandaruwan[1] · Nadeesha Madugalla[2] · Madurya Adikaram[2] · Amarasooriya Pitawala[1,3] · Tharanga Udagedara[4]

Chaturanga Sandaruwan
chaturangasandaruwangbcs@gmail.com

Madurya Adikaram
maduryaadikaram@seu.ac.lk

Amarasooriya Pitawala
apitawala@pdn.ac.lk

Tharanga Udagedara
tharanga@uwu.ac.lk

[1] Postgraduate Institute of Science, University of Peradeniya, Peradeniya 20400, Sri Lanka

[2] Department of Physical Sciences, Faculty of Applied Sciences, South Eastern University, Sammanthurai 32200, Sri Lanka

[3] Department of Geology, Faculty of Science, University of Peradeniya, Peradeniya 20400, Sri Lanka

[4] Department of Applied Earth Sciences, Faculty of Applied Sciences, Uwa Wellassa University, Badulla, Sri Lanka